

**REVIEW OF THE MECHANICAL PROPERTIES OF
LUNAR SOILS**

BY

JAVEN S. FIGUEROA

Bachelor Of Science In Civil And Environmental Engineering
University Of Central Florida
May 1998

Submitted To The Department Of Civil And Environmental Engineering In
Partial Fulfillment Of The Requirements For The Degree Of

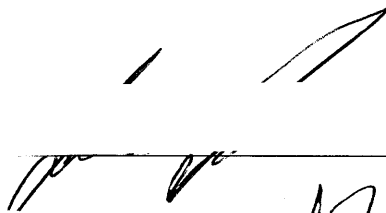
Master of Engineering in Civil and Environmental Engineering at the
Massachusetts Institute Of Technology

June 1999

Copyright © 1999 Massachusetts Institute Of Technology

All Rights Reserved

Signature of Author _____



Javen S. Figueroa

May 7, 1999

Certified By _____

Associate Professor of Civil and Environmental Engineering

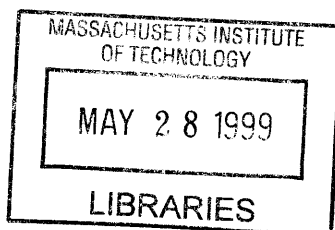
Andrew J. Whittle

Thesis Supervisor

Approved By _____

Chairman, Departmental Committee On Graduate Studies

Andrew J. Whittle



ARCHIVES

REVIEW OF THE MECHANICAL PROPERTIES OF LUNAR SOILS

By Javen Figueroa

Submitted to the Department of Civil and Environmental
Engineering on May 7th, 1999 in partial fulfillment of the
requirements for the Degree of Master of Engineering in Civil
and Environmental Engineering

ABSTRACT

This thesis summarizes the history of lunar soil exploration through the Surveyor and Apollo programs, 1966 – 1972. Our current knowledge of the physical and engineering properties of the lunar regolith is derived mainly from measurements made on bulk and core samples returned to earth, as well as trenching, penetration and simple geophysical experiments performed during the five successful Apollo missions to the moon. Most of this data corresponds to material in the upper 1 to 3 m of the lunar surface.

Lunar regolith is comprised of a mixture of basalt, impact melt glasses, breccias and agglutinate particles, and is derived from processes related to surface impacts and volcanic activity. The soil itself has a particle size distribution that resembles a well graded silty sand with angular particles and often containing a significant fraction of crushable (hollow) glass spheroids and agglutinates. The soil typically has a specific gravity of 3.1 and is found at an average porosity of approximately 45 – 50 %. The material has both cohesive and frictional components of shear strength, the former presumed to be related to electro-static forces between particles.

Recent Space Exploration Initiatives have motivated the development of simulants that replicate quite closely the average properties of lunar regolith. These materials provide the basis for future lunar and Martian exploration and construction priorities.

Thesis Advisor: Andrew J. Whittle

Title: Associate Professor of Civil and Environmental Engineering

TABLE OF CONTENTS

<i>Table of Contents</i>	3
<i>List of figures and tables</i>	4
<i>Acknowledgments</i>	7
1. INTRODUCTION	8
2. LUNAR SOIL EXPLORATION AND RECOVERY: 1966 – 1972.	10
2.1. AN INTRODUCTION TO LUNAR GEOLOGY	10
2.1.2. <i>Microcraters</i>	12
2.2. LUNAR SOIL TYPES	13
2.3. LUNAR SOIL STRATIGRAPHY	15
2.4. OVERVIEW OF LUNAR SOIL EXPLORATION.....	16
2.3.1. <i>Surveyor</i>	16
2.3.2. <i>Apollo</i>	17
2.3.2.1. Apollo 11	19
2.3.2.2. Apollo 12.....	20
2.3.2.3. Apollo 14.....	21
2.3.2.4. Apollo 15.....	21
2.3.2.5. Apollo 16.....	22
2.3.2.6. Apollo 17.....	23
2.4. INSTRUMENTATION	23
2.4.1. <i>Surveyor Program</i>	24
2.4.2. <i>Apollo program</i>	26
2.4.2.1. Core Sampling.....	28
2.4.2.2. In-situ Tests	30
2.4.2.3. Other field observations	31
FIGURES.....	34
TABLES.....	58
3. ENGINEERING PROPERTIES OF LUNAR SOILS	61
3.1. PHYSICAL CHARACTERISTICS OF RETURNED LUNAR SOILS	62
3.2. SHEAR STRENGTH PARAMETERS	66
3.3. DEFORMATION PROPERTIES.....	72
FIGURES.....	76
TABLES.....	87
4. EXPERIENCE WITH LUNAR SOIL SIMULANTS	91
4.1. SELECTION OF SIMULANTS	91
4.2. APPLICATIONS OF SIMULANTS.....	93
FIGURES.....	97
TABLES.....	102
5. SUMMARY AND CONCLUSIONS	103
REFERENCES	106

LIST OF FIGURES AND TABLES

<i>Number</i>		<i>Page</i>
Figure 2-1	Impact between the Earth and a Mars-sized body	34
Figure 2-2	The near and far sides of the moon	35
Figure 2-3	Lunar geological timeline	36
Figure 2-4	Cratering process	37
Figure 2-5	Ejection process	38
Figure 2-6	Microcraters	38
Figure 2-7	Breccias and basaltic rocks	39
Figure 2-8	Agglutinates	40
Figure 2-9	Spherical glass particles	40
Figure 2-10	Apollo 12 core tube	41
Figure 2-11	Lunar exploration timeline	16
Figure 2-12	Surveyor 1 lunar module	42
Figure 2-13	Lunar geographical features	43
Figure 2-14	Lunar landing sites	44
Figure 2-15	Sea of Tranquility	45
Figure 2-16	Ocean of Storms	45
Figure 2-17	Fra Mauro Crater	46
Figure 2-18	Hadley Rille/Apennine Mountains	46
Figure 2-19	Descartes	47
Figure 2-20	Taurus-Littrow	47
Figure 2-21	Soil Mechanics Surface Sampler	48
Figure 2-22	Surveyor 3 testing layout	48
Figure 2-23	Surveyor color chart	49
Figure 2-24	Surveyor 3 bearing and impact test results	49
Figure 2-25	Modularized Equipment Transporter (MET)	50
Figure 2-26	Lunar Roving Vehicle (LRV)	50
Figure 2-27	Terrestrial sampling tubes	51
Figure 2-28	Apollo core tubes	51
Figure 2-29	“Buzz” Aldrin driving sample tube with hammer	52
Figure 2-30	Apollo Self Recording Penetrometer (SRP)	52
Figure 2-31	SRP – Upper housing assembly and recording cylinder	53
Figure 2-32	Astronaut conducting trench test	53
Figure 2-33	Correlation of footprint depth vs. porosity	54

Table 2-1	Particle size distributions of lunar soil samples	55
Table 2-2	Surveyor 3 bearing and impact test results	55
Table 2-3	Summary of porosity estimates	56
Table 2-4	Pre-Apollo strength property estimates	56
Table 2-5	Apollo strength property estimates	57
Figure 3-1	Apollo 11 particle size distribution curve	73
Figure 3-2	PSD curves for Apollo 11/12/13 and 14	73
Figure 3-3	Angular terrestrial sand	74
Figure 3-4	Porosity/Void Ratio/Relative Density relationship	75
Figure 3-5	Mohr-Coulomb strength envelope	76
Figure 3-6	Stability numbers	76
Figure 3-7	Penetration resistance vs. depth	77
Figure 3-8	Apollo 15 strength parameters from trench and penetration tests	78
Figure 3-9	Laboratory penetration test	79
Figure 3-10	Miniature triaxial apparatus	80
Figure 3-11	Direct Shear test results	81
Figure 3-12	Curved strength envelope	82
Figure 3-13	Strength envelopes for lunar soils and basaltic lunar simulants	82
Figure 3-14	Shear wave velocity estimates	83
Figure 3-15	Results of vacuum oedometer tests	83
Table 3-1	Specific gravity test results	84
Table 3-2	Density measurements	85
Table 3-3	Best estimates of density vs. depth	85
Table 3-4	Measured min. and max. densities	85
Table 3-5	Strength parameters from SRP	86
Table 3-6	Summary of laboratory penetration tests	86
Table 3-7	Vacuum direct shear test results	86
Table 3-8	Miniature triaxial test results	87
Table 3-9	Miniature direct shear results	87
Table 3-10	Recommended values of strength parameters	87
Table 3-11	Recommended values of compressibility parameters	87
Figure 4-1	PSD curves for Apollo samples and lunar soil simulants	94
Figure 4-2	Penetration test results for simulants	95
Figure 4-3	Penetration results on simulants at varying g levels	96
Figure 4-4	Disturbance in core tube samples	97
Figure 4-5	PSD of JSC-1 lunar soil simulant	97
Figure 4-6	Mohr circles for JSC-1 in CD triaxial compression test	98

Table 4-1	Comparison of soil properties for lunar soil and lunar soil simulant	99
Table 4-2	Properties of JSC-1 and lunar soil	99

ACKNOWLEDGMENTS

First and foremost, I would like to thank my parents Richard and Millie. Without their love and support, I could not be the person I am today. Evan and Jolie, thanks for being my ever supportive siblings. I also wish to thank the family and friends who have been there for me throughout my life.

I must give thanks to the people who have supported me in my studies at MIT. Professor Andrew Whittle deserves my utmost gratitude for the time and effort he contributed to making sure my thesis was completed on time and in good form. I want to thank Professor Ladd for teaching me so much about soils and geotechnical engineering. Lastly, I must thank Professor Connor and Charles Helliwell for their guidance during the HPS project and throughout the year.

If I forgot anyone, thank you too.

1. INTRODUCTION

The Moon is Earth's only satellite. This makes the Moon and studies concerning it an extremely important scientific topic. Understanding how the moon was formed brings us closer to a better understanding about the formation of the Earth, as well as the rest of the solar system. The Earth and the Moon have been paired for approximately 4.6 billion of years, and their effect on each other is of great importance. Furthermore, man has an innate desire to push and expand as far as technology and dreams will let him. Exploration of the Moon, once a child's dream, became a reality in the late 1960's. What is Man's next step?

Colonization of the lunar surface is an appealing idea for many reasons. For example, because the moon always faces the earth from the same side, the far side of the moon would provide a location almost free of the earth's electromagnetic influence. A lunar outpost would not only give scientists a chance to study the moon to greater lengths, but would also provide for a better position with which to study the rest of the universe. Furthermore, the moon could become a source of material and energy. Aluminum and Iron are abundant within lunar mineral. Helium, Hydrogen and Oxygen can also be found in lunar minerals, all of which could act as fuel for sustaining life in lunar bases (Heiken et al., 1991).

The design and construction of a lunar outpost presents many challenges, but as on earth, understanding the properties of the ground conditions is always an important factor.

Our knowledge current knowledge of lunar soils is derived mainly from the Apollo Space Program's lunar exploration, 1969 through 1972. Soil tests were run in-situ and on samples returned to earth. The purpose of most of these studies was to aid in the improved design of instrumentation and vehicle design for future missions. However, with the implications of lunar colonization in mind, a question stands. Is the existing lunar soil data sufficient for reliable construction of lunar facilities?

This thesis reviews the scope of the lunar soil exploration program conducted by NASA, focusing mainly on the Surveyor and Apollo programs. Chapter 2 summarizes the background information concerning the space program, lunar surface geology, soil sampling and testing information, as well as observational methods used to interpret soil properties. Chapter 4 presents an overview of research concerning the properties of lunar soil simulants. This chapter also addresses the usefulness of lunar simulants in making estimates of lunar soil properties. Finally, a brief discussion of the results will be made, along with recommendations for further study in light of future lunar construction.

2. LUNAR SOIL EXPLORATION AND RECOVERY: 1966 – 1972.

2.1. AN INTRODUCTION TO LUNAR GEOLOGY

A good understanding of lunar geological history is essential in helping us create the most complete picture about the moon and its soils. While the moon is the Earth's closest celestial body, surface characteristics could not be further apart. Likewise, the processes that dictate the formation of lunar and terrestrial surfaces are also highly dissimilar. Both weather and water dominate the Earth's geological processes. The Moon has neither. The Lunar surface, completely barren of fluid water and with almost no atmosphere, has been shaped by a completely different sequence of events. Most of these events took place in the distant past (approximately 4.0 billion year ago) of the moon's long history (Heiken et al., 1991).

The origin of the moon is a topic still under debate (Heiken et al., 1991). There exist two 'classical' views concerning the formation of the moon. The first postulates that the moon and earth were formed together as sister planet while the second considers that the moon was captured by the earth's gravitational field. A third theory has been proposed more recently by Hartmann and Davis (1975), based on data acquired by the space program. This theory states that the Earth was subject to a collision with a body about the size of Mars. The result of this collision was both the combination of the metallic cores of the two bodies, but also the formation of an orbiting mass. This mass, along with the small debris and dust drawn in over the years,

would form what we know as the moon. Figure 2-1 displays the impact proposed by the “Impact” theory. The figure clearly shows the collision of Mars sized body with the earth (small and large circular shapes). The result of this impact is the almost complete combination of the metallic cores of the two bodies and the ejection of a large mass that would eventually form the moon (Heiken et al., 1991).

Figure 2-2 displays the current state of the moon (near and far sides). The darker areas on the moon are known as maria, or seas, while the lighter shaded area are cratered highlands known as terrae. The maria areas were formed by volcanic activity caused by impacts. The craters in the terrae are older structures associated with much earlier volcanic activity.

Figure 2-3 presents a proposed lunar geological timeline. The age of the moon is estimated at 4.6 billion years, while the formation of the maria area didn’t occur until approximately 3.8 billion years ago. Furthermore, apart from the occasional impacts, little has changed on the lunar surface since this heavy volcanic activity.

It should be noted that due to the earth’s geological nature and processes, the surface has changed very considerably throughout its history. This fact makes the moon even more desirable to study, since it’s relatively unchanged surface in the last 3 billion years acts like a window to study the past, without the obscuring influence of weather, water, etc.

The most dominant formational process on the surface of the moon is due to cratering (Figure 2-4). The large impacts in the moon's history and continual small-scale bombardment today have caused the surface to be blanketed in overlapping layers of impact ejecta. This layer of mixed ejecta covering most of the lunar surface is known as the lunar regolith.

Figure 2-5 illustrates the cratering and ejection processes. Material size and continuity is a function of the distance from the impact area and the impact magnitude. Any one location on the lunar surface has been a different distances from impacts and therefore has a large mix of particle sizes and types. An equation has been proposed (McGetchin et al., 1973) which relates the thickness of ejecta, **t**, as a function of distance from crater center, **r**, and diameter of crater, **D**. The equation is defined as follows:

$$t = 1.7 \times 10^{-3} r^{-3} D^{2.74}$$

2.1.2. MICROCRATERS

It should be evident from Figure 2-2 that craters exist in many different sizes throughout the surface of the moon. However, there are also craters that cannot be seen, except on the smallest of scales. Microcraters, on the surface of small particles, are widely found in particulate material on the moon's surface. Figure 2-6 displays different microcraters on the surface of particles. Due to impacts such as these, any volcanic material that pooled on the surface

approximately 3.8 billion years ago immediately started to be broken down. The constant bombardment of the lunar surface by small particles and by charged solar wind makes the lunar surface extremely hostile. For this reason, lunar construction may require underground facilities. These types of facilities could utilize lunar materials as a means of blocking harmful projectiles and energy. However, subsurface construction would require more detailed knowledge concerning soil properties than would the alternative above ground facilities. Possibilities such as this increase both the desire and need to accurately characterize the lunar surface and soils.

2.2. LUNAR SOIL TYPES

As stated above, lunar and terrestrial formation processes differ in many ways and hence, the lunar regolith is expected to differ from terrestrial soils. The first and most obvious difference is the lack of any pore fluids in lunar soils. The lunar regolith contains a mixture of particle sizes ranging from fines to large rocks and boulders. Figure 2-7 summarizes some of the particle size distributions from various lunar samples. The fifth digit of each sample refers to the type, i.e. 0 – Unsieved < 10-mm fines, 1 – < 1-mm sieved fraction, 2 – 1-2-mm sieved fraction, 3 – 2-4-mm sieved fraction.

Basaltic rock, or igneous rock, is one of the major two components of lunar rock formations. These rocks are primarily the result of volcanic activity on the lunar surface. Due to the high levels of basaltic material in the lunar

soils, it can be inferred that the impact processes were responsible for distributing basaltic rock material throughout the lunar surface. The second most plentiful type of rock materials are called breccias. These rocks are mixtures of other rock types bonded together from partial melting. Together, these rock types constitute the largest proportions of the returned Apollo mission samples. Figure 2-7 shows various types of basaltic and breccia rocks. Lunar soils are primarily composed of fragments and particles of these two elements. However, the lunar soils do include some other unique components.

One of the major unique components of lunar soil and rock material in the lunar regolith are agglutinates. These particles are aggregates of smaller particles, usually joined with melted glass. These particles formed from melting and micrometeor impacts such as those discussed above. Pictures of some lunar agglutinates are shown in Figure 2-8. Agglutinates are important in dating lunar soils, since the more agglutinate material present gives an indication of how long the soil has been exposed (Heiken et al., 1991).

Impact glasses are another unique component of lunar soils. These glass particles often form spherical beads and are found in a variety of colors. Orange and green being the most notable colors, due to their chemical composition. The glass particles are also known to contain entrapped gases. During compression testing, some of these particles will crush and release the gas. The presence of these particles can also cause a “ball bearing” or rolling type effect at low loads. However, large loads, such as those from men, 200 kg, or lunar vehicles, 75 – 708 kg, will be too high for slippage or rolling effects to be of any concern. At higher loads such as these, the spherical particles will simply be crushed. Apollo astronauts did notice a slight effect due to these

particles on their space walks (Heiken et al., 1991). Figure 2-9 shows different spherical glass particles, one with microcraters present.

2.3. LUNAR SOIL STRATIGRAPHY

The stratigraphy of the lunar soil is of major concern to scientists and engineers. Lunar foundation construction or excavation will require accurate data concerning the stratigraphy and especially the depth to bedrock. To date, however, lunar surface sampling equipment has only managed to probe to a maximum depth of 3m (Apollo 17 mission). An example of a typical driven core sample is shown in Figure 2-10. The core clearly shows layers with defined boundaries, representing impact ejecta from different regions. Furthermore, the only areas where bedrock has been observed are at the sides of deep crater walls. It is clear that mapping of the lunar bedrock, especially in the maria regions, is an area in which further scientific study is required.

2.4. OVERVIEW OF LUNAR SOIL EXPLORATION

On September 12, 1959, the Soviet Union launched the first lunar impact probe, Luna 2. Fueled by scientific interest and, more importantly, cold war competition, the United States would soon begin an aggressive program of lunar exploration. In 1964, the U.S. sent the first impact probe, Ranger 7, to the lunar surface. Soon thereafter, the Russians launched a series of lunar landers, prompting the U.S. to begin the Surveyor program, which provided the first direct data on lunar soils. Following Surveyor came Apollo, and the famous Apollo 11 moon landing. An outline of the Surveyor and Apollo programs can be seen below in Figure 2-11. The following sections review the scope of soil exploration in the Surveyor and Apollo programs.

2.3.1. SURVEYOR

The Surveyor program began in 1966 with Surveyor 1 and lasted through 1968, with Surveyors 3/5/6 and 7. The Surveyor missions were valuable tools in giving scientists data concerning the lunar surface and soil conditions without the need for direct human involvement. For the most part, the Surveyor

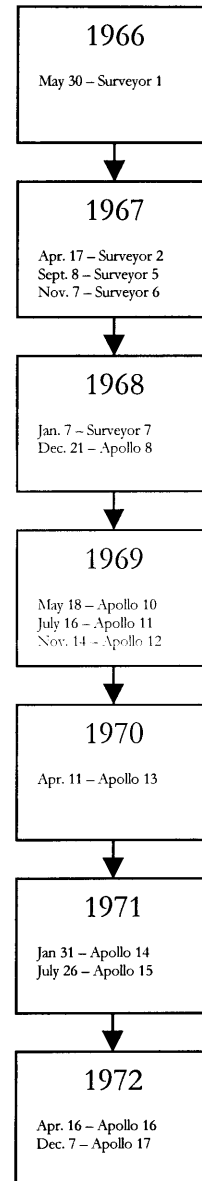


Figure 2-11

landing sites were chosen because they were being evaluated as possible Apollo landing sites. This fact made soil testing a critical task in the Surveyor missions. Until the landing of these modules (Figure 2-12), scientists and engineers did not know what to expect from the lunar surface. Each of the five successful Surveyor missions included soil mechanics experiments of some kind. These experiments included strain gauges, bearing and trenching experiments, and impact tests. The results of these tests will be discussed in further detail in Chapter 3. The locations of the Surveyor landing can be seen in Figure 2-14.

2.3.2. APOLLO

The Apollo space program began in 1966 with Apollo 8, climaxed in 1969 with the Apollo 11, the world's first manned landing on the moon, and lasted until 1972. Altogether, there were 9 successful Apollo missions¹. Of these, only Apollo 11 through 17 included manned space landings. However, in just these six missions, NASA collected 382 kilograms of rocks, pebbles, sand and dust. Furthermore, the program sought to evaluate the lunar surface for its inhabitability and possible material mineral wealth. However, even with preliminary tests and evaluation completed during the Surveyor program, scientists were still uncertain as to how the lunar environment would respond to the Apollo astronauts. Consider the following excerpt:

¹ The Apollo 13 mission was aborted due to a series of technical problems.

Just a few months before the flight of Apollo 11, it was seriously suggested that, when Astronaut Armstrong took his first steps on the lunar surface, the soil would jump onto his spacesuit because of the electrostatic attraction. The resulting coating of the soil covering his suit was expected to be so thick that he would not be able to see and might not be able to move. Then, if he were able to stagger back into the LM, there was concern that the highly reduced soil would burst into flames when the cabin was repressurized with pure oxygen. (Heiken et al., 1991)

It is clear that, until touchdown, some scientists had no idea what to expect from the lunar surface and its soils.

Various in-situ and lab tests were run in conjunction with the Apollo program. The tests and instrumentation used at each landing site will be discussed in Chapter 3. The landing sites for the Apollo program were chosen in order to maximize the information on different areas of the moon. The locations of the Apollo moon landings are shown in Figures 2-13 and 2-14. Although there is some variability in the soil conditions at each of these sites, this thesis emphasizes the commonality in the properties of the lunar regolith materials. The soil exploration taken place on each Apollo mission is summarized in the following paragraphs.

2.3.2.1. APOLLO 11

Apollo 11 was and still is the pinnacle of the Apollo space program for its achievement for mankind. From a geotechnical point of view, it provided the first samples of lunar regolith. The landing site, the Sea of Tranquility (a volcanically formed maria) The site was selected as a flat and relatively safe landing area, Figure 2-15. Most people know or have heard Neil Armstrong's famous first words as he stepped out of the lunar module onto the surface. However, few people know about the words that follow.

I'm at the foot of the ladder. The LM footpads are only depressed in the surface about 1 or 2 inches, although the surface appears to be very, very fine grained, as you get close to it, it's almost like a powder; down there, it's very fine...I'm going to step off the LM now. That's one small step for man. One giant leap for mankind. As the – The surface is fine and powdery. I can – I can pick it up loosely with my toe. It does adhere in fine layers like powdered charcoal to the sole and sides of my boots. I only go in a small fraction of an inch. Maybe an eighth of an inch, but I can see the footprints of my boots and the treads in the fine sandy particles. (Heiken et al., 1991)

Neil Armstrong
Tranquility Base, July 20, 1969

Various tests were conducted on the lunar surface. Core tube samples as well as bulk samples were taken and returned to laboratories on earth. A total of 21.6 kg of lunar soil and rock was returned to earth. However, much of the preliminary assessment of lunar soils were based on observations, such as insertion of flagpoles, depth of astronaut bootprints, reaction of soil to takeoff, etc. (Costes and Mitchell, 1970). Laboratory data from tests on the Apollo 11 samples were used to help NASA scientists to improve the testing equipment and collection methods used in later missions.

2.3.2.2. APOLLO 12

The second Apollo mission saw a few changes in the surface sampling and testing procedure. First and most importantly, the lunar sampling core apparatus was changed. While the Ocean of Storms (Figure 2-16) is located some distance from the Sea of Tranquility, the returned samples had a very similar composition. The location of this landing was also chosen to be near to the landing of Surveyor 3 (1967). Surface tests included checking the condition of the Surveyor module for the effects of its two-year stay. The results showed microcratering on certain glass parts, but for the most part, the equipment was unaffected (Heiken et al., 1991). As with Apollo 11, samples were taken with tongs, scoops, and a hammer driven core tube (Carrier et al., 1971). The total amount of samples recovered, including samples taken from the Surveyor module scoop, totaled 34 kg.

2.3.2.3. APOLLO 14

Having landed twice in a relatively flat maria area, the Apollo scientists felt it was time to obtain information about different types of terrain. Apollo 14 landed on the Fra Mauro formation, a hilly region close to the Apollo 12 site. (Figure 2-17) One of the primary objectives for this mission was to obtain geological information for a site close to a crater, the Fra Mauro Crater (Heiken et al., 1991). Obtaining information concerning the nature and formation of the lunar regolith was also a top priority. As with the Apollo 12 mission, sampling and instrumentation of the lunar surface evolved for the Apollo 14 exploration. This mission included the use of instrumentation new to lunar surface testing. Along with the procedures used in previous missions, Apollo 14 included simple penetrometer experiments, soil mechanics trenching and a modularized equipment transporter. The location of this landing gave the astronauts a chance to take samples with more rocky compositions, as opposed to the large fine quantities in the previous low-land areas. However, soil properties and composition still did not vary significantly. Apollo 14 astronauts brought back 36 kg of soil and rock samples.

2.3.2.4. APOLLO 15

Apollo 15 was the first of the more advanced and landed on a site that was chosen due to its apparent complexity. The location is on the boundary between the Apennine Mountain region and local mare areas of Hadley Rille,

Figure 2-18. This was also the first mission to employ the use of the Lunar Roving Vehicle (LRV). This made navigating around the lunar surface faster, giving the astronauts more time to perform tests and collect samples. Furthermore, this mission was the first to employ the use of the Apollo lunar surface drill core. The design of the drive core tube also evolved significantly, to lessen the impact of sample disturbance (see section 2.4.2.1). The new self-recording penetrometer was also used on this mission, adding to the quality of returned information. All together, Apollo 15 returned 82 kg of rocks and soil, along with the most comprehensive in-situ test results of any mission to date.

2.3.2.5. APOLLO 16

Apollo 16's primary objective was to obtain information about the formation of the highland area Descartes, Figure 2-19. Prior to the mission, this area was believed to be volcanic in origin. However, upon exploration and sample return, the area was found to be almost all impact melts and breccia material (Heiken et al., 1991). Additions to the lunar surface exploration program included the sample scoop and self-recording penetrometer with 3 different cone attachments. Variation of properties in lateral and vertical directions were also a priority on this mission, with greater area coverage due to the LRV. Also conducted were typical trenching tests, plate load tests, and observations of LRV wheel/soil and LM footpad/soil interactions. Apollo 16 returned a total of 95.7 kg of soil and rock samples.

2.3.2.6. APOLLO 17

Apollo 17 was the final mission of the Apollo program and the last occasion when humans have explored the lunar surface directly. The Taurus-Littrow Valley, Figure 2-20, was again chosen as the landing site, in order to investigate the boundary between maria and highland areas (similar to rationale for Apollo 15). Newly employed on this mission was a LRV mounted drill core, which obtained core samples up to 3.3m deep. Soil compositions, textures and colors were similar to the conditions at the other Apollo sites. However, differences in density with depth indicate different depositional history from the similar sites of Apollo 15 and 16. A total sample weight of 110kg was returned, including volcanic and impact breccia rocks as well as soil containing orange glass particles.

2.4. INSTRUMENTATION

The instrumentation and sampling equipment used in the Surveyor and Apollo missions had a large effect on the accuracy of the geological data acquired. Soil exploration was limited by the payloads of the lunar exploration modules. Therefore, choosing the proper equipment for each mission was critical. As with any type of study, the information obtained in the early tests helped to improve the testing on later missions. Surveyor data, along with tests on lunar soil simulants, helped scientists and engineers to make choices

concerning the tools and instruments used on the Apollo missions. Likewise, early Apollo missions led to changes in the tools used in later Apollo missions. This section summarizes the site instrumentation and robotic tools used in the lunar landings. Laboratory tests and procedures on the returned soil samples will be discussed in Chapter 3.

2.4.1. SURVEYOR PROGRAM

Estimations of lunar surface/soil properties on the Surveyor missions were conducted using the following methods:

- 1- Pictures from spacecraft cameras
- 2- Response of spacecraft landing gear to impact
- 3- SMSS (Soil Mechanics Surface Sampler) data

Surveyor 1 employed only the first two methods for the return of surface and soil information. However, due to the success of Surveyor 1 and the need for better soil data, Surveyor 3 was equipped with the SMSS (Scott and Roberson, 1968). The SMSS was originally designed only to sample the lunar soils at the landing site, but was later altered to conduct soil mechanics tests as well. The apparatus (Figure 2-21) is made up of an arm capable of extension, contraction, and movements to the left, right, up and down. The end of the arm holds scoop with a movable door. Two small motors located in the Surveyor module power the sampler. Sensing equipment on the sampler

included (1) a strain gauge mounted on the arm to measure the force acting on the sampler; (2) another strain gauge located near the bucket/scoop to measure the contraction force of the arm; and (3) an accelerometer attached to the bucket's cutting edge used to measure its decelerations during impact with the surface (Scott, 1967).

The sampler was capable of conducting the following:

- 1- Static Vertical Bearing/Penetration Tests
- 2- Static Drag/Horizontal Load Tests
- 3- Impact Deceleration Tests
- 4- Weighing Experiments
- 5- Alpha Scatter Experiments

Bearing tests were conducted with the scoop on the surface of the site and at the bottom of various dug trenches. This gave scientists an indication of the resistance profile of the regolith. Impact tests were also conducted on the surface and inside of trenches for the purpose of measuring vertical variability of soil properties. Since the Surveyor lander was immobile after landing, all of these tests had to be conducted within the range of arm movement (152-cm radius). The test layout for the SMSS on the Surveyor 3 craft is shown in Figure 2-22. The device made crude weight measurements that were only sufficient to differentiate between a solid or relatively porous material. The

Surveyor scoop was also used to pick up and move the α -scatter device to different locations. This device provided information concerning the atomic properties of the lunar surface.

The module was also equipped with a color chart on the landing gear. Soil could be dumped from the scoop onto the reflective surface of the footpad, and its basic color could be compared a key chart (Figure 2-23).

A summary of the penetration tests for Surveyor 3 is shown below in Table 2-2. Plots of this data show that for the bearing tests, there does not seem to be any relationship of applied force with depth. In the case of the Impact tests, some correlation may be made, although the data has a large amount of scatter, Figure 2-24.

Nevertheless, the data could represent any amount of unknowns attributed to the lunar surface conditions and/or instrument error. More data with larger applied loads and higher drop heights would be needed to establish any reliable correlation.

2.4.2. APOLLO PROGRAM

The instrumentation used by astronauts in the Apollo program went through significant changes between each mission. The sampling techniques, core tube design and in-situ tests gradually became refined and consequently, more and better data was received. The following paragraphs evaluate some of

the sampling and in-situ testing techniques employed by the Apollo astronauts, with comparisons to terrestrial practice wherever applicable.

Apollo astronauts conducted their sampling in two different ways. The first and most simple sampling method was to collect bulk samples from the surface using scoopers and/or tongs to grab material. This material was then placed in vacuum sealable bags attached to the astronaut equipment packs. Because an astronaut's pack was out of his own reach, this exercise was done in pairs.

The need for sample material was obviously a very high priority on the lunar missions. Procedures such as these would probably not be employed on earth, undisturbed samples being much more desirable. However, the equipment and time on the moon was limited. Therefore, even highly disturbed bulk samples such as these were of great use to the multitude of scientists involved in the project, including geotechnical engineers. Changes in equipment throughout the Apollo project included extension of sampling equipment handles for ease of use and innovations to increase mobility. Mobility of the astronauts during their missions was extremely important in being able to get as much data from the different areas as possible. Apollo 11 astronauts were made to carry instruments on their space suits. A hand tool carrier was used by Apollo 12 astronauts to ease the burden of the instrumentation. It should be noted that the safe storage and transport of these instruments was extremely important. Almost all of the surface sampling and testing equipment had the potential to rip or puncture astronaut suits and hoses if not careful. Apollo 14 increased the portability of the

instruments even further by adding a Modularized Equipment Transporter or MET (Figure 2-25) to the payload.

This device was basically a rickshaw on which the hand tool carrier was mounted. Large changes in mobility took place on the Apollo 15 mission with the addition of the LRV, Lunar Roving Vehicle (Figure 2-26). This happened to coincide with the addition of new lunar instrumentation, such as the Apollo self recording penetrometer. The LRV was employed on the rest of the Apollo missions. The Apollo 17 mission made one final addition to the sampling equipment, with the LRV mounted core sampler. This allowed astronauts to take samples while en-route to different areas.

2.4.2.1. CORE SAMPLING

The second type of sampling technique used by Apollo astronauts on all missions was core sampling. Terrestrial core sampling is traditionally done with some type of thin-walled tube, such as a Shelby tube (Figure 2-27) which is usually jacked into the ground. Apollo mission employed these types of sampler, but not until Apollo 15. In the earlier missions (Apollo 11 through 14) thick-walled samplers were used. As is the case on Earth, these samplers increased the amount of disturbance and decreased the amount of soil recovery in the tubes.

Evaluating the effectiveness of different tube sizes is commonly done by looking at the Area Ratio (AR), which is a function of the inner and outer tube diameters (Houston and Mitchell, 1971):

$$AR = \frac{D_o^2 - D_i^2}{D_i^2} \times 100$$

The area ratios for different core tubes were calculated and tested on lunar soil simulants exhibiting similar properties to the lunar soil. Basaltic silty sand was used as a simulant for the study (Houston and Mitchell, 1971). Tubes with lower Area Ratio's, and hence thinner walls, exhibited much better performance. However, these observations were not reflected in early designs. Figure 2-28 shows the cross-sections of the different core tube designs used in the Apollo program.

The Apollo 11 core tube (Figure 2-28) had an inward flare which caused severe disturbance. The design of this flare is the opposite of samplers found on Earth. Apollo 12 – 14 saw improvements to the design that helped lower disturbance, but the sampler was still very thick-walled. The AR for these samplers is about 140 % compared to 14 % for a common terrestrial sampler. It wasn't until the Apollo 15 core tube that the design became closer to that of a thin-walled tube on Earth, the AR being reduced to 7.4% (Figure 2-28). Another improvement in the design for Apollo 15 was the removal of the follower from the end of the sampler. In the early sampler, this follower was pushed down with the tube to prevent soil from coming out of the end. However, if too much force were applied, the sample would become severely

disturbed (Carrier et al., 1971). Another factor contributing to disturbance was the driving method. If the resistance to hand pushing the tube became too high, the astronaut would proceed to hammer the tube to advance it (Figure 2-29).

The Apollo 15-17 missions were equipped with a drill core tube. This type of sampling would eliminate much of the human error involved in driving and disturbance due to hammering. This type of core also solved some of the penetration problems the astronauts were having with the driven tubes. As the depth of the sample increased, so did the frictional resistance on the tube surface. Therefore, there seemed to be a limit to the depth which the tubes could be driven. However, using the drill core, the astronauts were able to retrieve the deepest samples of the project. The maximum sample depth achieved was about 3 meters. The modified drive cores and the drill cores utilized on Apollo 15-17 returned the least disturbed and deepest samples of the entire Apollo project.

2.4.2.2. IN-SITU TESTS

The Apollo surface exploration program utilized two in-situ tests for characterization of soil properties. The first of these two were penetration tests. The penetrometer equipment went through two different designs in the Apollo program. Apollo 14 was the first to utilize such as test, called the Apollo Simple Penetrometer or ASP. This instrument had no moving parts and penetration distances were measured by calling out stripes on the side (Heiken

et al., 1991). A more elaborate model, the Self-Recording Penetrometer or SRP, was used on the Apollo 15 and 16 missions. The tool had three different cone attachments and a plate attachment for measuring soil resistance (Figure 2-30). The gold recording cylinder had the etchings of the penetration data inscribed in it and was the only part of the instrument returned to earth (Figure 2-31). This tool is very similar to terrestrial cone penetrometers and was just as useful in making estimates of soil strength and variations with depth.

Trenching tests were also a common practice on the Apollo missions. The trenches could be used to take bulk samples and perform tests at depth (Figure 2-32). Secondly, observations of the depth of trenches before collapse could be made. From this information, estimates of the soil's cohesion and friction angle could be made (corresponding to assumed Mohr-Coulomb shear strength parameters). Many estimates of these parameters were made, which shall be discussed further in later sections.

2.4.2.3. OTHER FIELD OBSERVATIONS

Apart from in-situ testing procedure, various observational techniques were used to make estimates of soil properties. As far back as the NASA Ranger missions, scientists were making estimates of the lunar surface properties based on pictures alone. Although these estimates were far from precise, they were sufficient in identifying possible upper and lower bounds of the soil properties. From the Ranger photographs, it was postulated that the

lunar surface was either composed of mostly hard volcanic rock or a very porous layer of soil of unknown depth. Using these estimates, the future Surveyor landers would either land safely on the surface or sink into the soil. It would seem that these estimates were little better than none at all. Nevertheless, scientists and engineers settled on an intermediate case, which turned out to be a good estimate of the actual conditions. Instead of taking the worst case scenario of a cohesionless granular soil with a porosity, $n = 90\%$, they chose one with $n = 50\%$. The success of the Surveyor program is a testament to the acceptable values the scientists chose (Scott, 1973). Photographs from the Ranger missions also included slopes angles. Estimates of soil strength were made from these pictures as well as with stability analyses on crater walls (Mitchell et al., 1972).

Estimates of soil properties on the Surveyor missions came from the response of landing gear to contact and the SMSS, as described above. The response of the soil to the lander's jets and engines also led to some estimates of strength properties (Table 2-3).

Porosity estimates were made from analysis of footprints and boulder tracks documented on the Apollo missions and the Lunar Orbiter missions respectively. Footprints were used to estimate porosity n the following manner:

1. Estimations of footprint depth from photographs.
2. Calibration of depths using lunar soil simulant.
3. Conversion of footprint depth to porosity using terrestrial tests on simulant material.

4. Development of empirical correlation for interpretation of n (Figure 2-33).

This 'design curve' was then used to convert footprint depth to porosity for imprints up to 15-cm deep. A total of 273 footprint depths were observed at the Apollo 11/12/14 and 15 sites. The data was compiled and analyzed to determine statistical variations (Houston et al., 1972).

Boulder track photographs from the Lunar Orbiter missions were also used to make estimates of porosity. Theoretical analyses conducted on the formation of boulder tracks as related to mechanical properties of soil is the foundation for these estimates. For 69 boulder tracks from 19 different locations, friction angles were calculated using an average cohesion value of 0.5 kN/m^3 . Relationships between friction angle and porosity were established using the lunar soil simulant LSS No. 2 (Houston et al., 1972), Section 4.2. For this data, a statistical analysis was conducted and estimates of porosity were made. A summary of porosity estimates from different locations is shown in Table 2-3.

Strength parameters were derived from a number of sources including but not limited to the methods described above. Summaries strength property estimates made both pre and during the Apollo missions are shown in Tables 2-4 and 2-5.

FIGURES

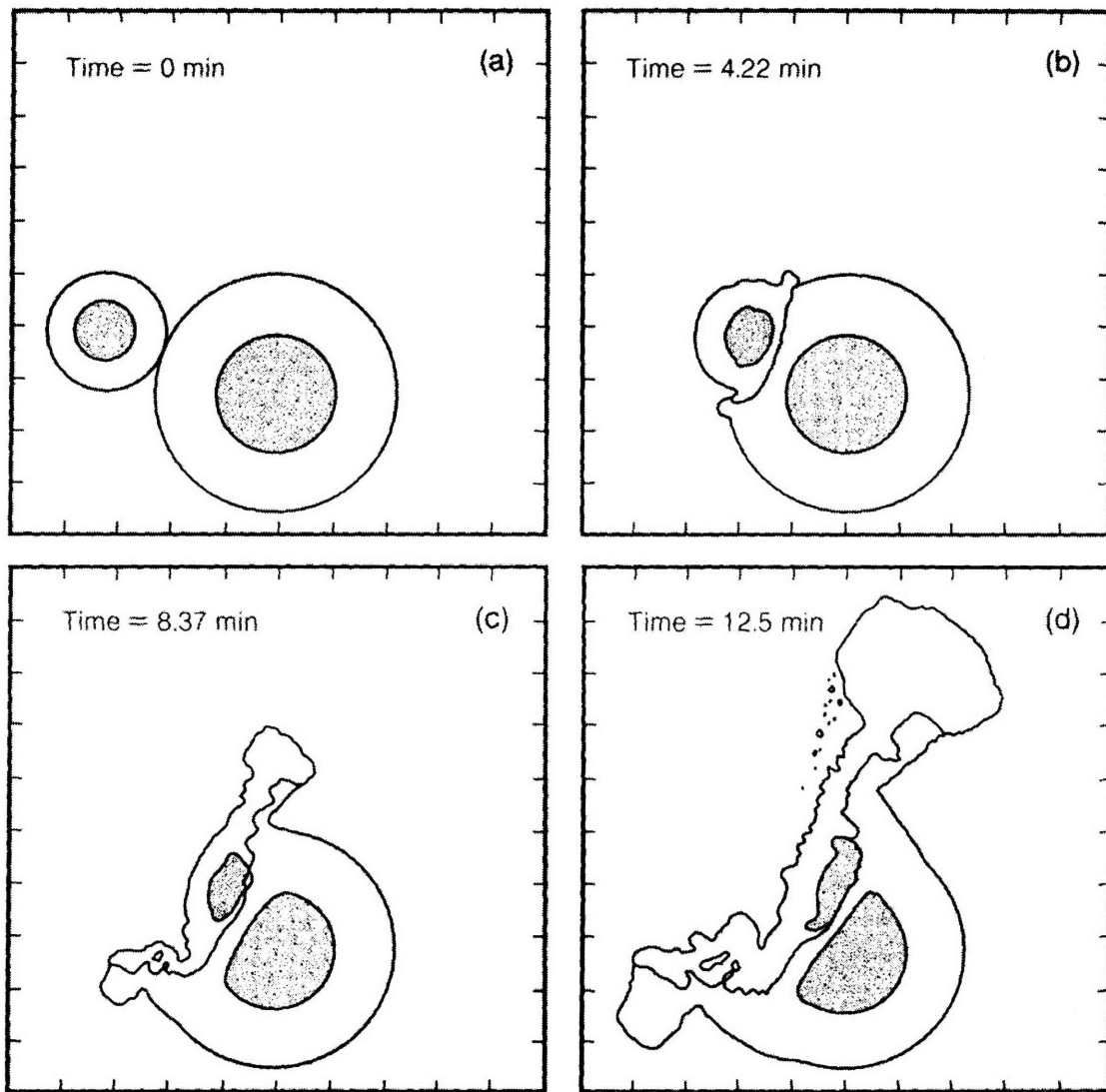


Figure 2-1 – Elapsed time of impact between the Earth and a Mars-sized body, leading to the formation of the moon (Heiken et al., 1991).

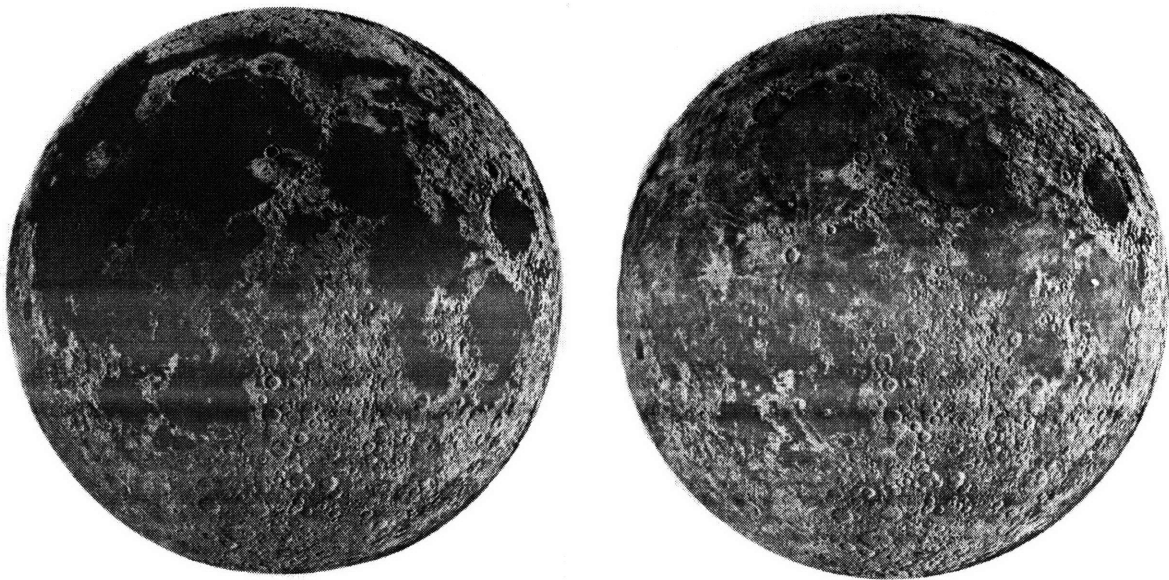


Figure 2-2 – The near (left) and far sides of the moon. The dark areas covering the near side of the moon are the maria formations. (Heiken et al., 1991)

Time Stratigraphic Units	Date Years	Rock Units	Events	Notes
COPERNICAN SYSTEM		Few large craters	Tycho Aristarchus	Craters with bright rays and sharp features at all resolutions
		Few large craters	Copernicus	Craters with bright rays and sharp features but now subdued at master resolutions
ERATOSTHENIAN SYSTEM	$3-2 \times 10^9$	Apollo 12 lavas	Eratosthenes	Craters with Copernican form but rays barely visible or absent
	$3-3 \times 10^9$	Apollo 16 lavas	Imbrium lavas	Few lavas with relatively fresh surfaces
IMBRIAN SYSTEM	$3-4 \times 10^9$	Luna 16 lavas	Eruption of widespread lava sheets on nearside; few eruptions on farside	Extensive piles of basaltic lava sheets with some intercalated impact crater ejecta sheets
		Mare lavas		
	$3-6 \times 10^9$	Apollo 11 lavas		
	$3-8 \times 10^9$	Apollo 17 lavas		
	$3-9 \times 10^9$	Cayley formation? Havellius Fm. Fra Mauro Fm.	Orientalis Basin Imbrium Basin	
NECTARIAN SYSTEM		Crisium Moscoviense Humorum Nectaris Serenitatis Smythii Tranquillitatis Nubium	Numerous overlapping large impact craters and associated ejecta sheets together with large basin ejecta	
PRE-NECTARIAN	$4-1 \times 10^9$			Any igneous activity at surface obscured by impact craters
	$4-6 \times 10^9$		Formation of moon	'Crystalline' rocks formed by early igneous activity

Figure 2-3 – Lunar geological timeline (Guest, 1977).

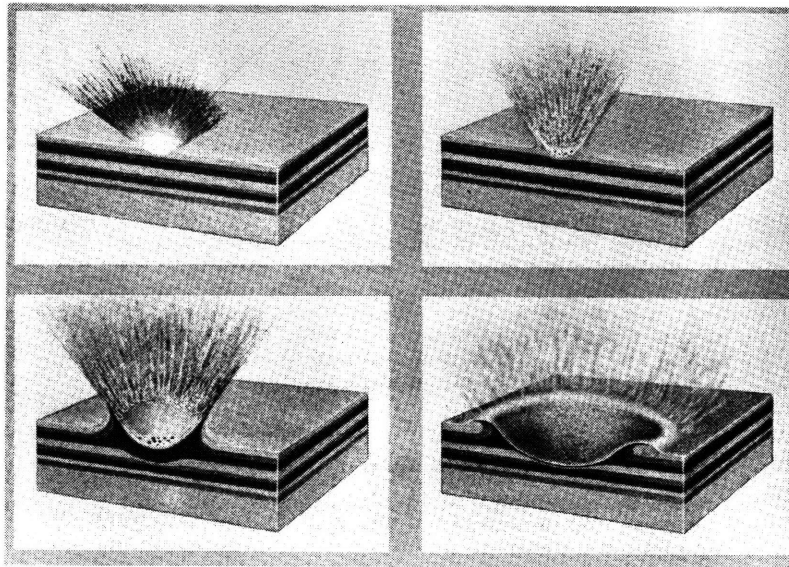


Figure 2-4 – The Cratering Process. Note the formation of outer rim and ejection of matter to surroundings. (Mutch, 1970)

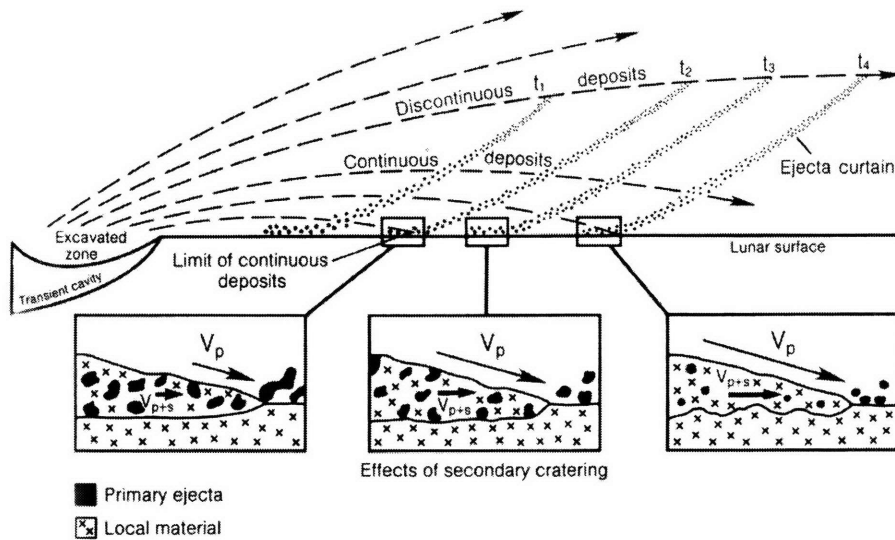
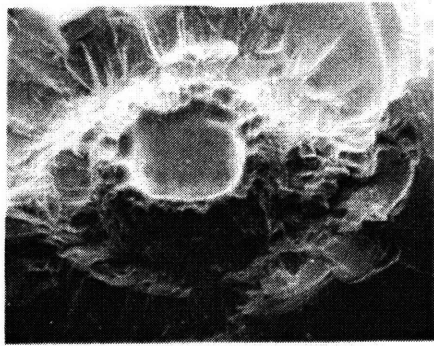
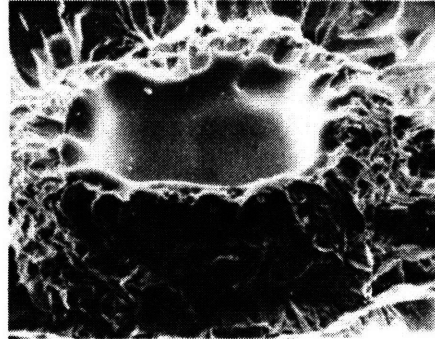


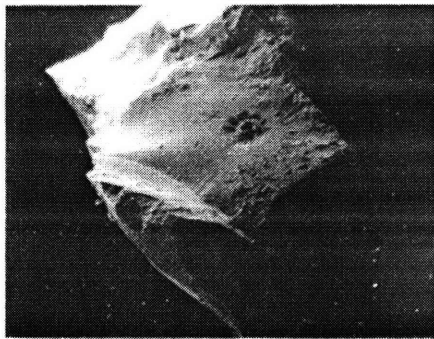
Figure 2-5– The Ejection Process. V_s = Velocity of impact ejecta;
 V_{s+p} = velocity of resultant debris surge (Heiken et al., 1991)



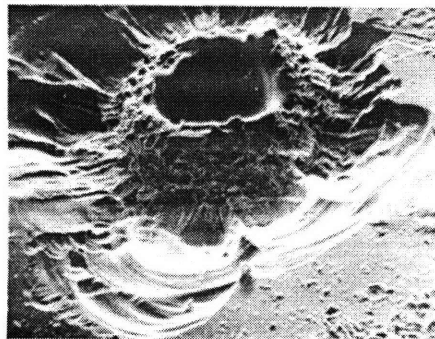
0.05 mm



0.025 mm



0.5 mm



0.05 mm

Figure 2-6– Scanning Electron Microscope pictures of Microcraters on the surface of lunar soil particles (Levinson and Taylor, 1971).

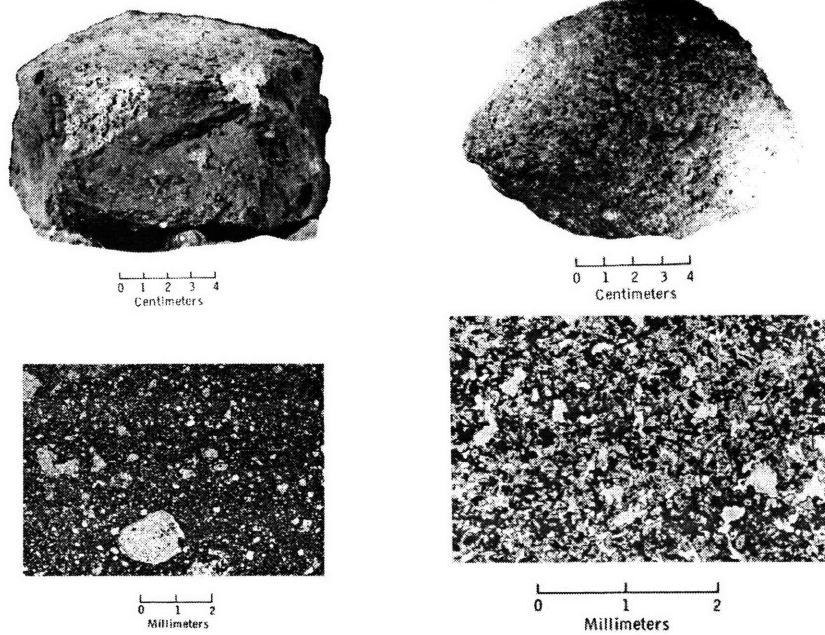


Figure 2-7 – Examples of Breccia (left) and Basaltic Rocks. Note the different particle sizes in cross-sectional slice of the breccia rock. (Levinson and Taylor, 1971)

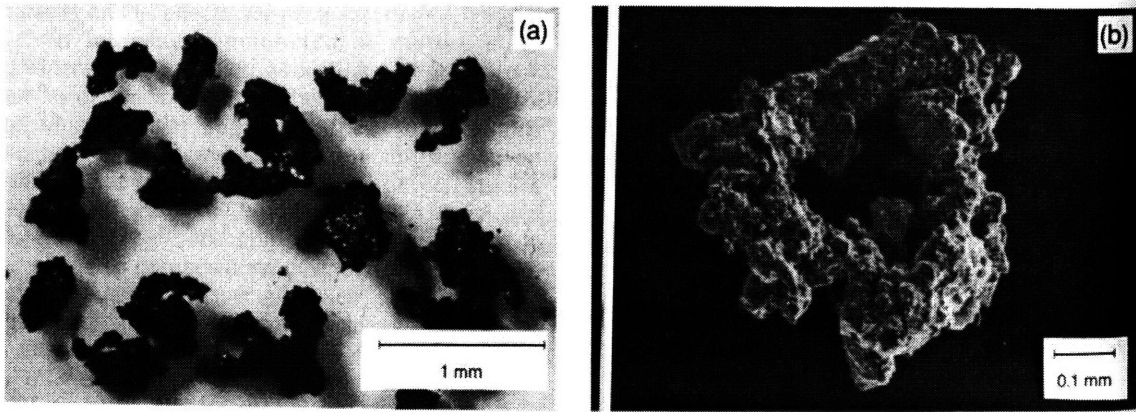


Figure 2-8 – Agglutinates (Heiken et al., 1991)

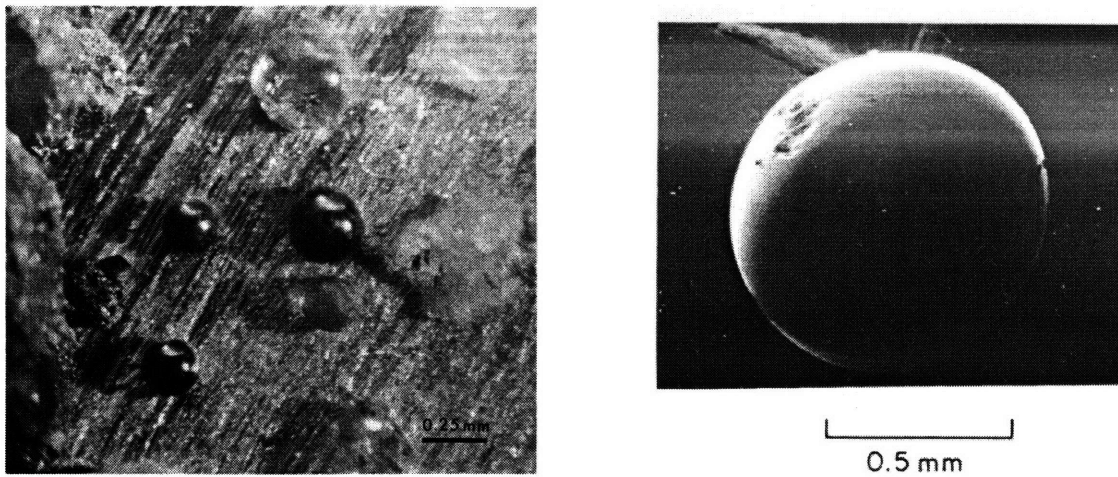


Figure 2-9 – Left – Assorted Glass Spherical Glass Particles, Right – Glass Sphere w/ microcrater (Muchth, 1970; Levinson and Taylor, 1971)

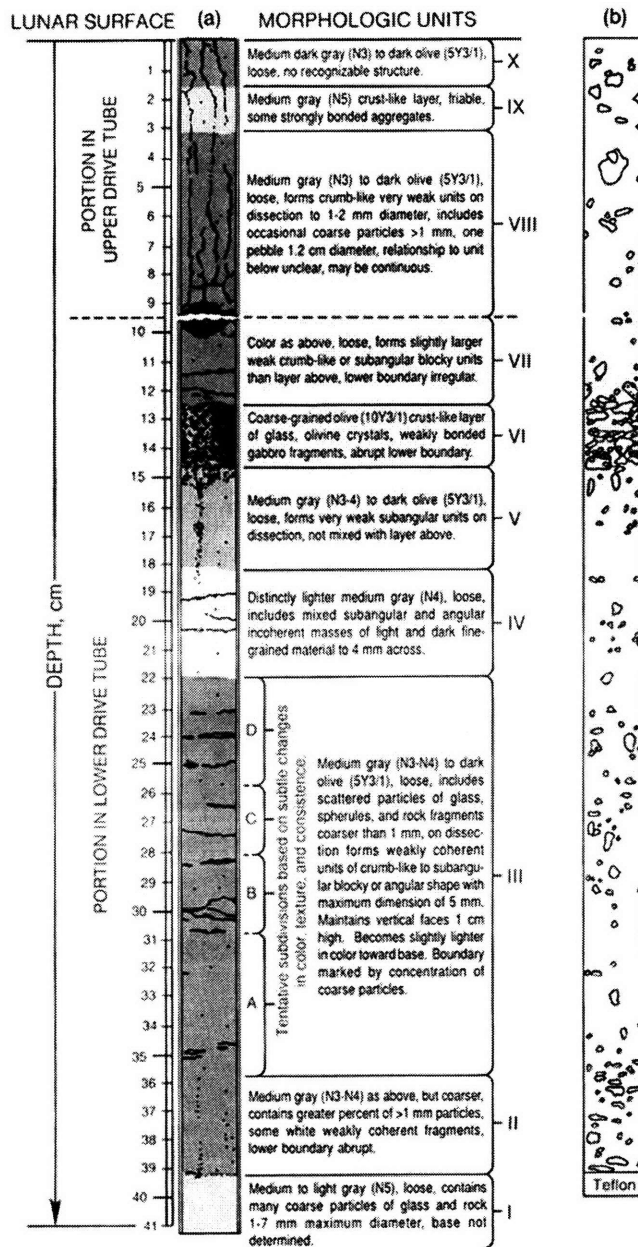


Figure 2-10 –Apollo 12 Lunar Core Tube sample.
(Heiken et al., 1991)

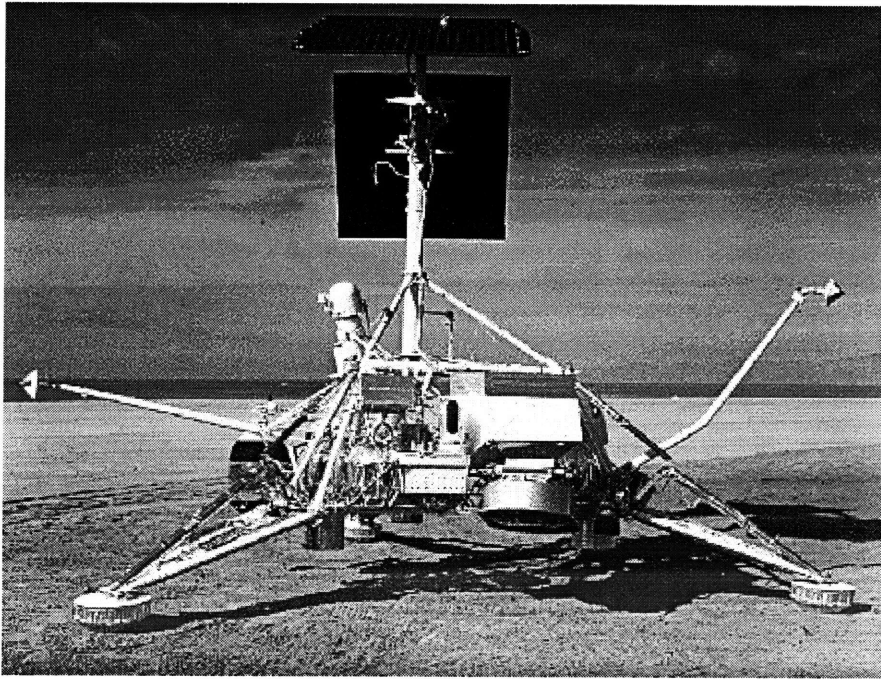


Figure 2-12 – Surveyor 1 Lunar Experiment Module

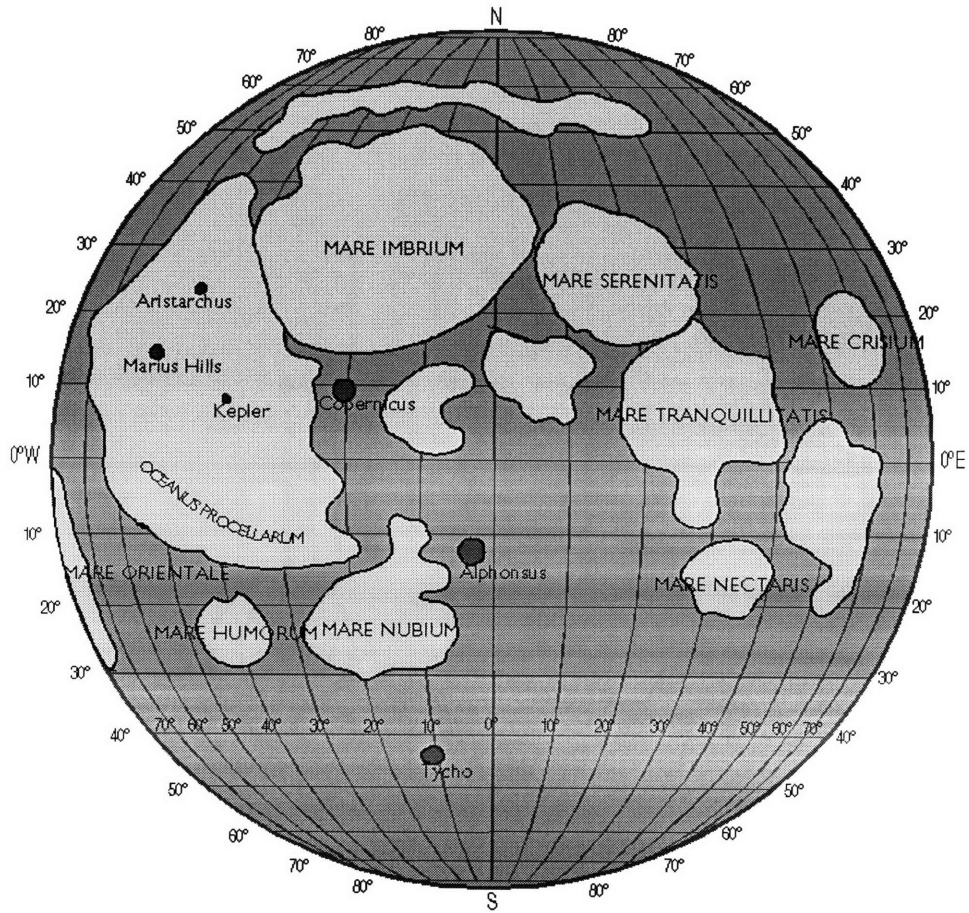


Figure 2-13 – The Lunar near side with important geographical features labeled

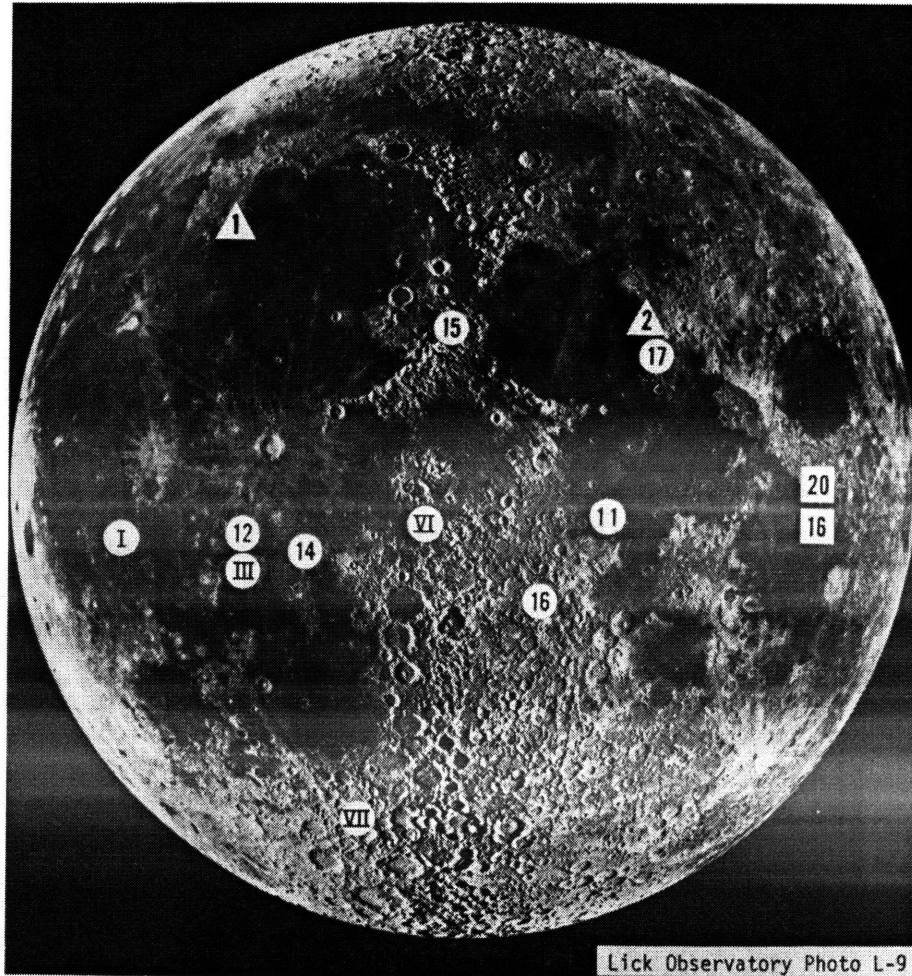


Figure 2-14 – Lunar Landing Sites. Circles w/ Arabic Numbers – Apollo, Circles w/Roman Numerals – Surveyor, Squares and Triangles- USSR Luna (Guest and Greeley, 1977)

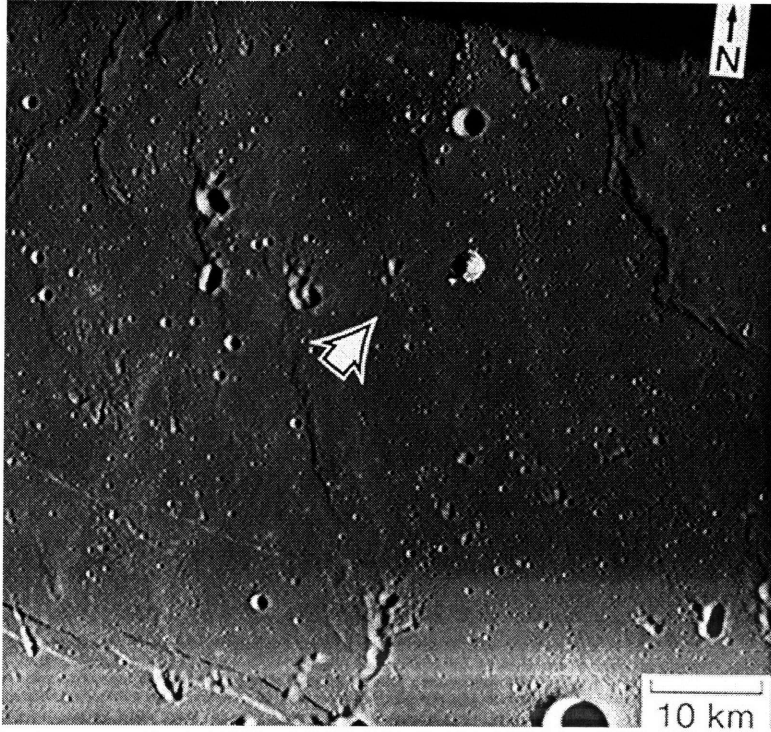


Figure 2-15 – Apollo 11 Landing Site – The Sea of Tranquility

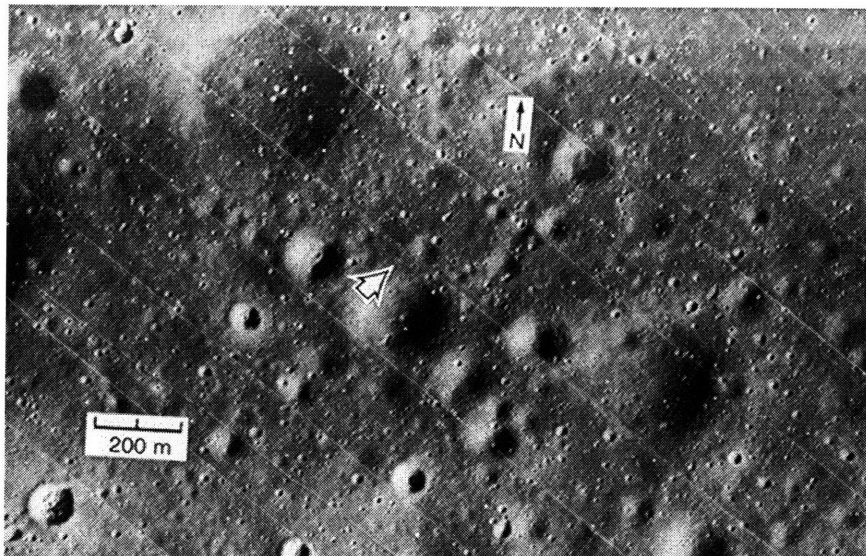


Figure 2-16 – Apollo 12 Landing Site – The Ocean of Storms

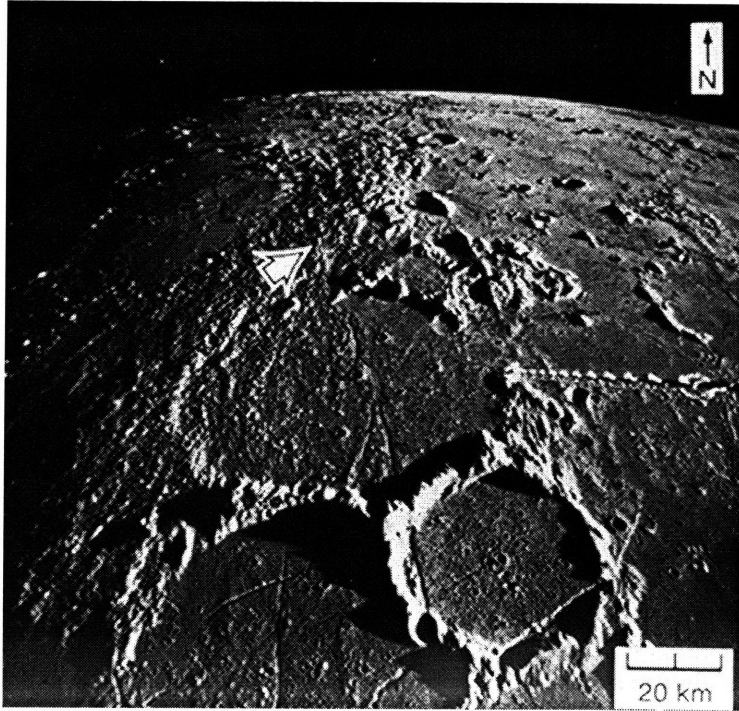


Figure 2-17– Apollo 14 Landing Site – Fra Mauro Crater

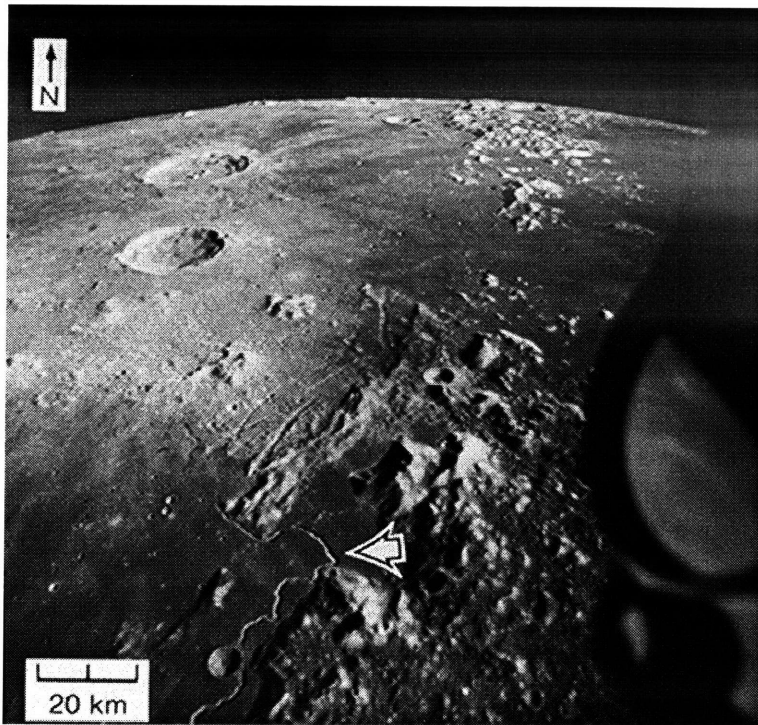


Figure 2-18 – Apollo 15 Landing Site – Hadley Rille/Apennine Mountains

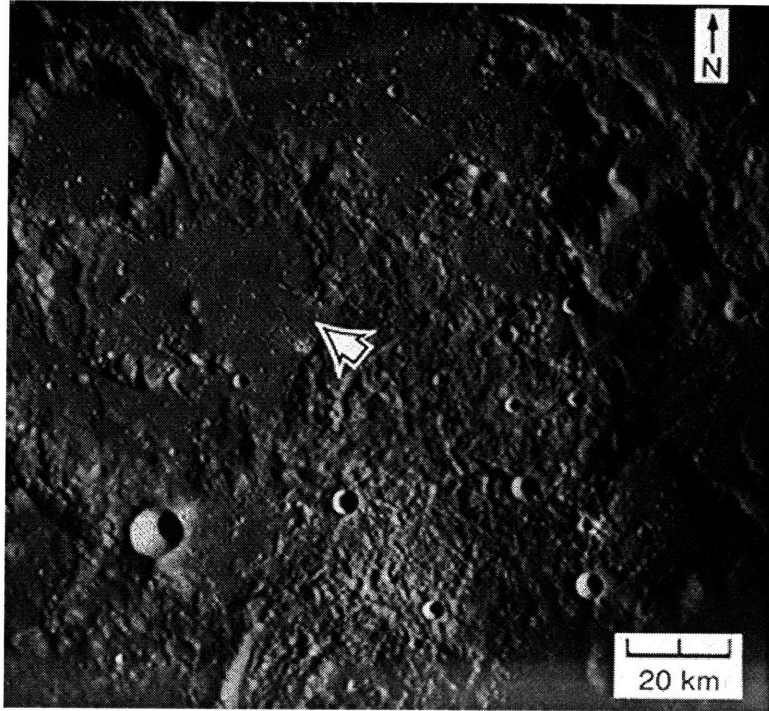


Figure 2-19 – Apollo 16 Landing Site - Descartes

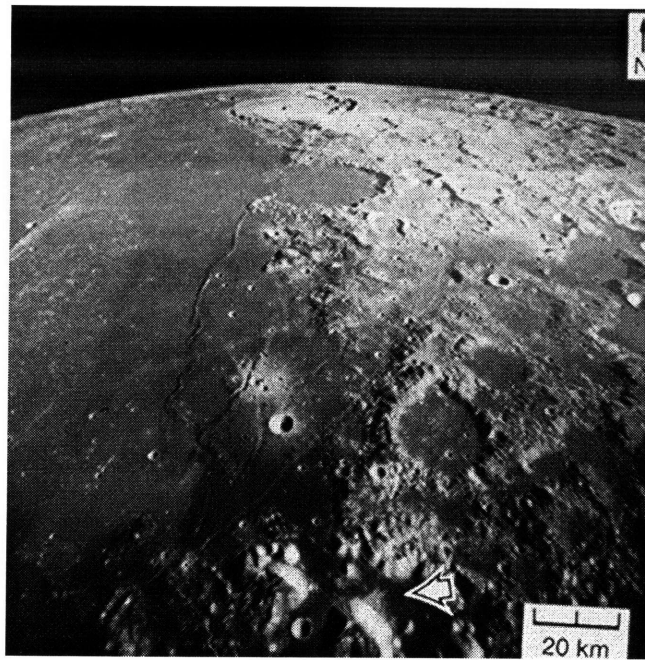


Figure 2-20 – Apollo 17 Landing Site –
Taurus- Littrow

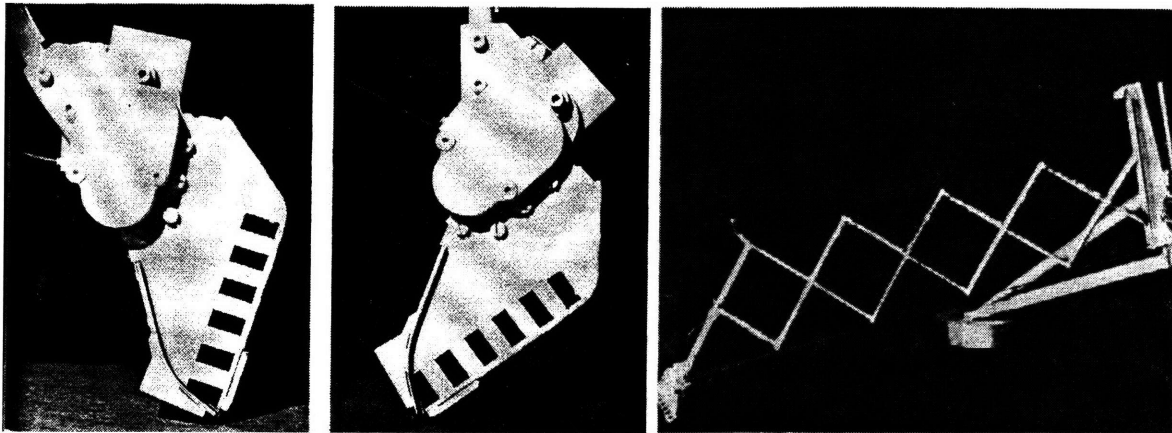


Figure 2-21 – Soil Mechanics Surface Sampler (SMSS), Arm Extension (Right) and Scoop (Left) (Scott, 1967; Scott and Roberson, 1968)

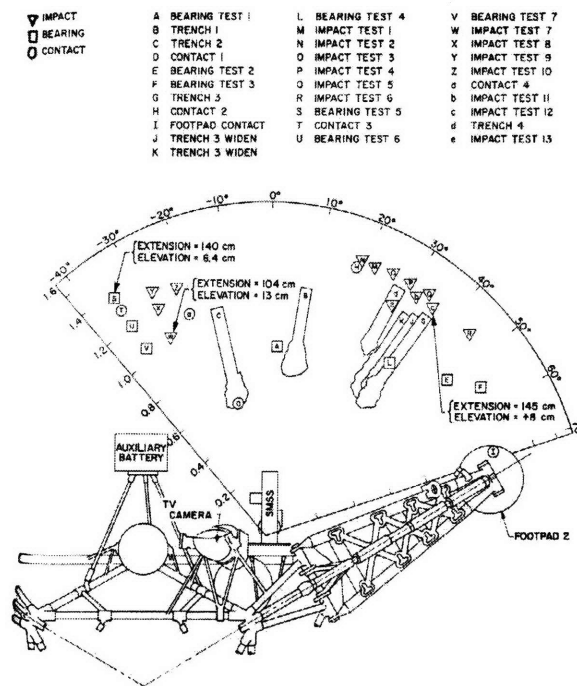


Figure 2-22 – Surveyor 3 Testing Layout (Scott and Roberson, 1968)

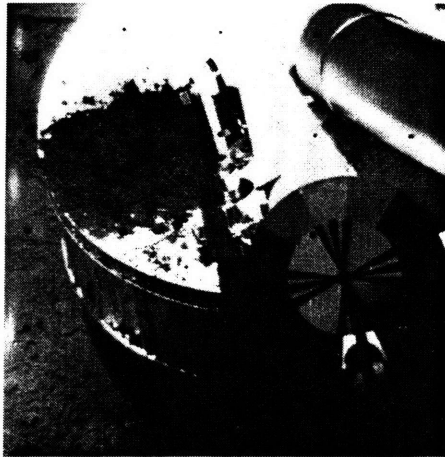


Figure 2-23 – Color Chart mounted to footpad of Surveyor lander.

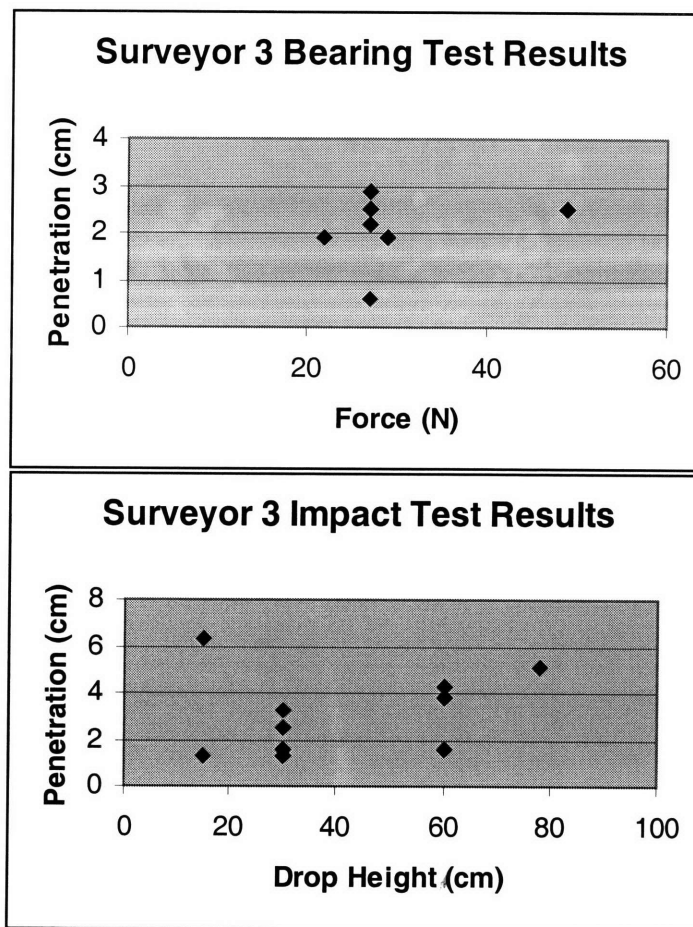


Figure 2-24 – Plotted results from Surveyor 3 Bearing and Impact tests.

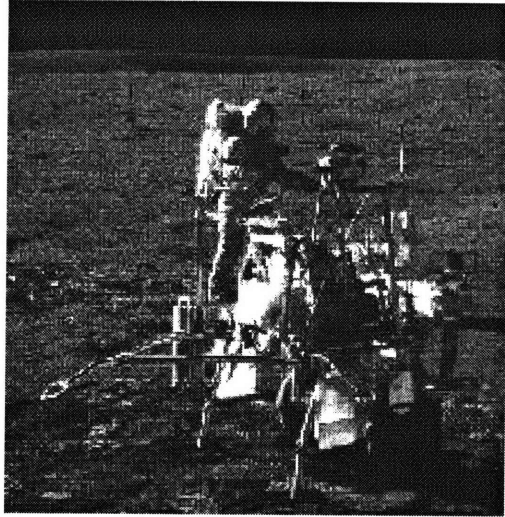


Figure 2-25 - Modularized Equipment Transporter w/ Astronaut in background.

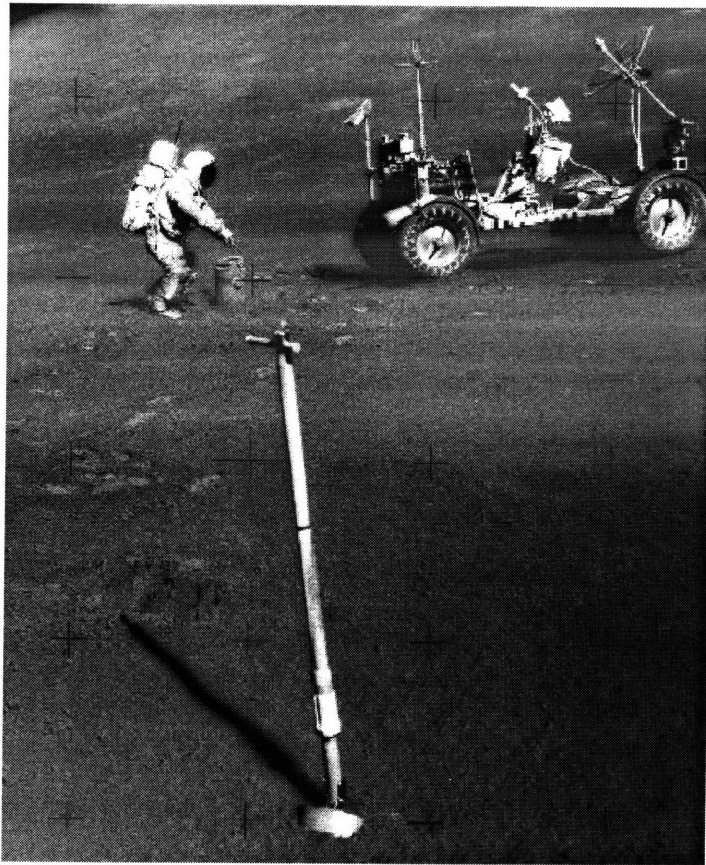


Figure 2-26 – Lunar Rover (background) with astronaut and sample scoop.

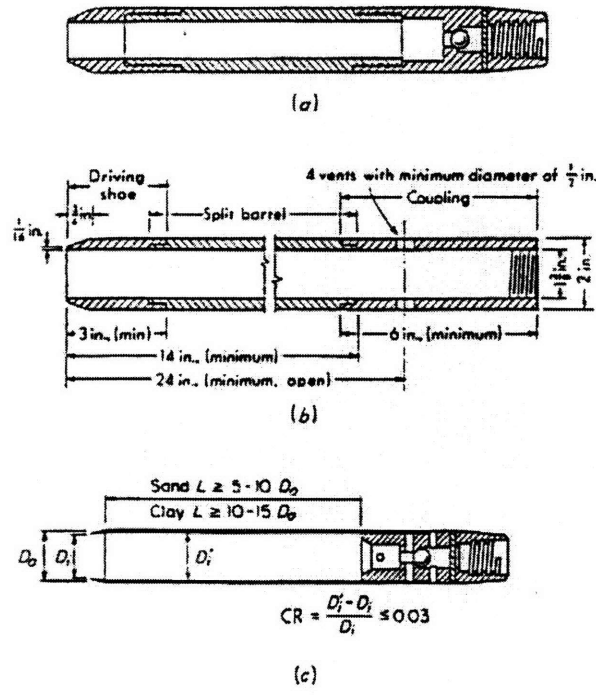


Figure 2-27 – Terrestrial Sampling Tubes. (a) Standard Split Spoon (b) Dimensions of standard split spoon assembly (c) Thin Walled/Shelby tube sampler

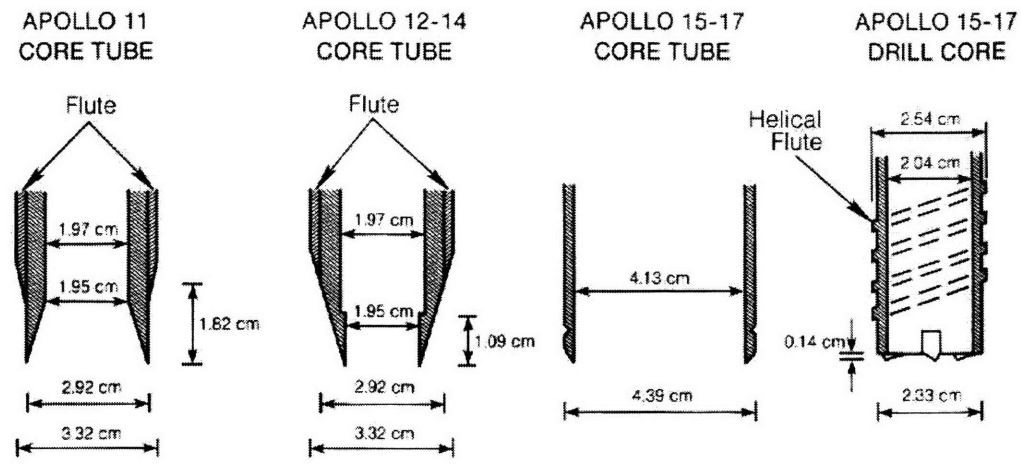


Figure 2-28 – Cross-Sections of Apollo Core Tubes (Heiken et al., 1991)



Figure 2-29 – Astronaut “Buzz” Aldrin driving sampling tube with hammer.

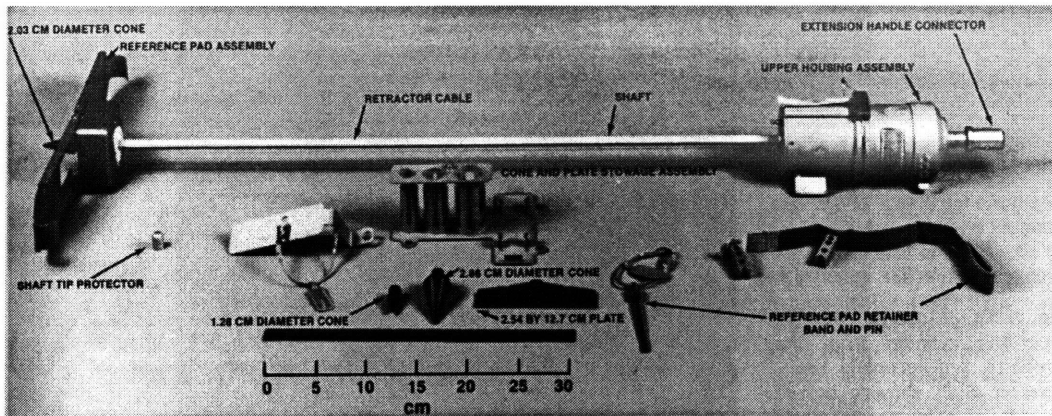


Figure 2-30 – Apollo Self-Recording Penetrometer shown with cone and plate attachments (Heiken et al., 1991).

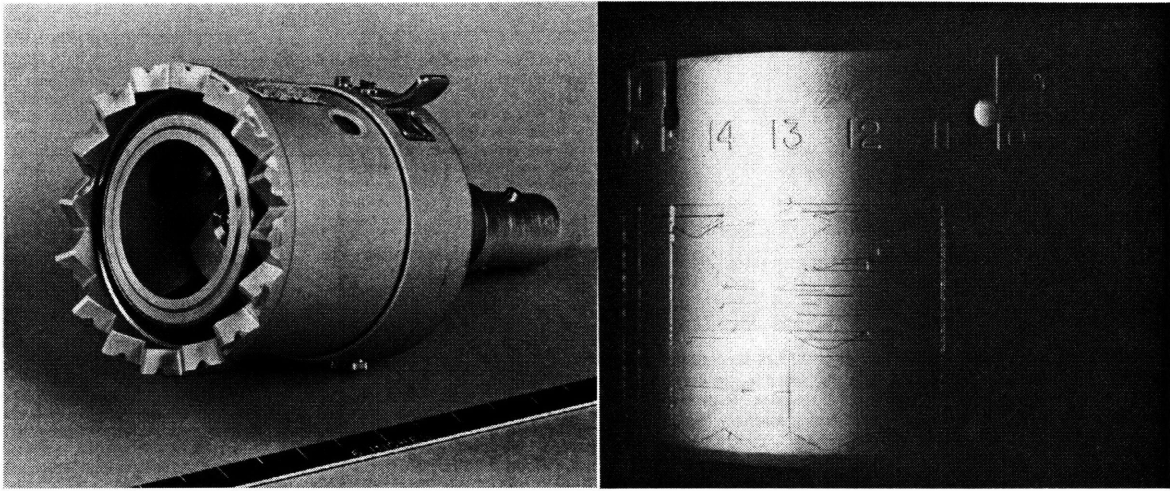


Figure 2-31 – Upper Housing Assembly (Left) and Recording Cylinder (Right) (Heiken et al., 1991)

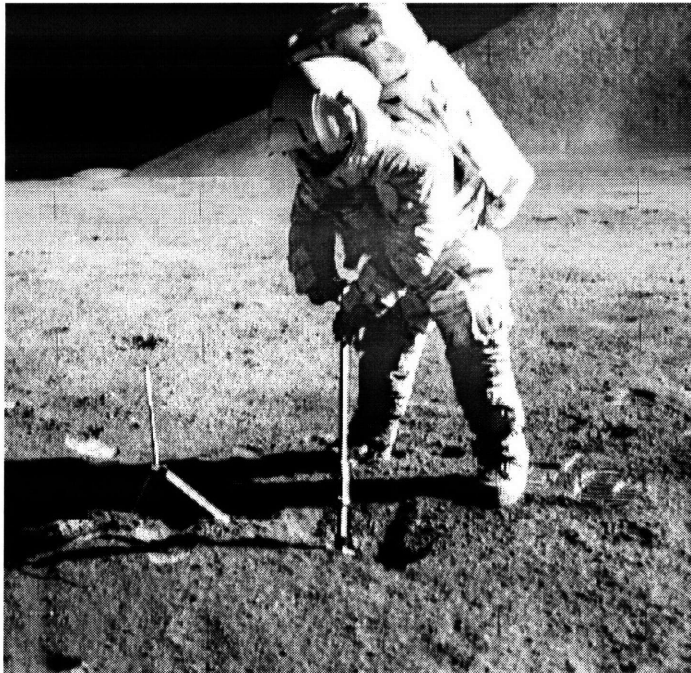


Figure 2-32 – Apollo astronaut conducting tests inside trench. Pictured left is a gnomon used to obtain information concerning coordinates and surface color.

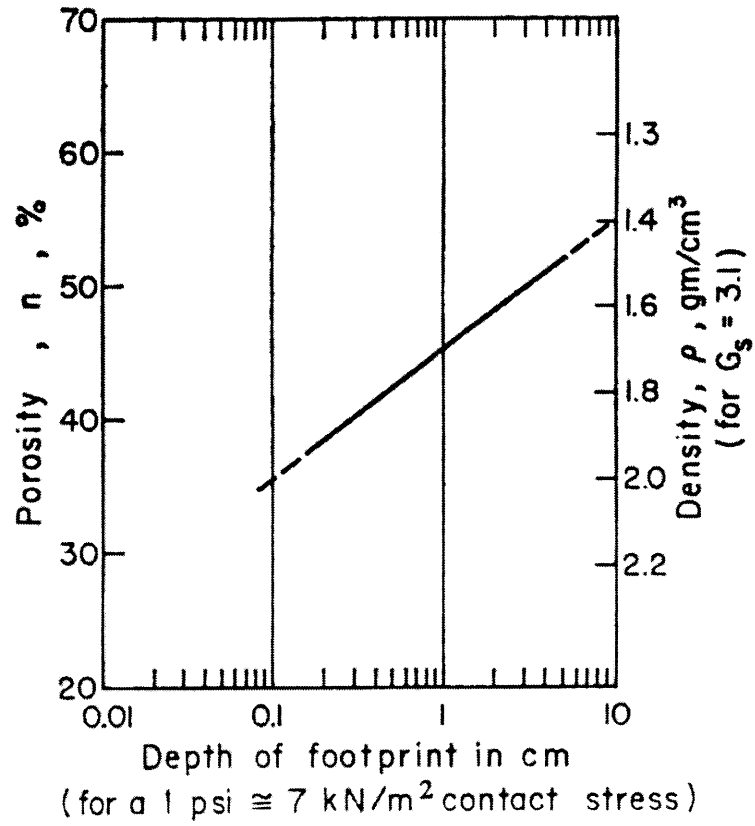


Figure 2-33 - Correlation of footprint depth with porosity. (Houston et al., 1972)

TABLES

	Soil Sample	Size Fraction					Mean Size, M_z	
		> 1 cm	4 - 10 mm (weights in grams)	2 - 4 mm	1 - 2 mm	< 1 mm	<1cm (μm)	<1mm (μm)
Apollo 11	10002	18.5	7.6	11	14.7	424.5		52
Apollo 12	12001		UNAVAILABLE					60
Apollo 14	14003	23	33	31.8	42.1	947.9	129	99
	14141	0	7.4	6.7	5.4	28.5	616	123
	14163	0	196.5	197.1	288.7	4444	76	56
Apollo 15	15220	0	7	5.8	2.4	290		43
	15270	0	4.4	13.7	20.7	798.3		94
	15400	513.1	7.9	6.1	4.8	86.4	330	61
Apollo 16	61180	0	6.1	6.2	9.4	156.2	94	64
	61220	5.1	10.6	9.6	6.4	61	216	68
	62280	12	14.3	13.1	21.7	218.5	134	70
	64500	31.2	24.2	24.1	28.4	495.7	104	65
	68500	1.3	17.3	25.1	37.8	521.1	106	68
Apollo 17	70180	466.6	1.7	3.1	4.6	157.1	67	58
	71500	52.3	13.1	17.6	22.7	600.9	83	65
	72140	1.3	2.7	1.9	5.3	225.9	57	50
	72500	3.1	8	12.9	24.1	687.2	67	57
	73240	1.6	22.3	14.4	14.9	192.7	127	51
	74220	0	0.98	0.17	0.68	7.77		41
	78220	0	1.5	2.7	5.2	227.1	50	45
	78500	109.3	19.2	16.1	21.4	718.7	46	41

Table 2-1 – Particle Size distribution of Lunar Soils (Heiken et al., 1991)

Test	Force (N)	Penetration (cm)	Drop Height (cm)
Bearing 1	49		2.5
Bearing 2	27		2.5
Bearing 3	22		1.9
Bearing 4	27		0.6
Bearing 5	27		2.2
Bearing 7	27		2.9
Bearing 8	29		1.9
Impact 1			1.3
Impact 2			3.3
Impact 3			2.5
Impact 4			3.8
Impact 5			4.3
Impact 6			3.8
Impact 7			1.3
Impact 8			1.6
Impact 9			1.6
Impact 10			1.6
Impact 11			6.3
Impact 12			6.3
Impact 13			1.3
Impact 14			5.1

Table 2-2 – Results of Surveyor 3 Bearing and Impact Tests

Data Source	Description	Number of Observations N	Mean Porosity n (%)	Standard Deviation s
Apollo 11	All data	33	43.8	2.2
	All data w/out Crater rims	30	43.3	1.8
	Crater rims only	3	48.4	2
Apollo 12	All data	119	43.8	3.6
	All data w/out Crater rims	88	42.8	3.1
	Crater rims only	31	46.5	4.8
	Near LM w/out Crater rims	28	43.9	2.5
Apollo 14	All data	42	43.9	2.3
	All data w/out Crater rims	38	43.3	2.2
	Crater rims only	4	50.1	2.9
Apollo 15	All data	129	43.6	2.8
	All data w/out Crater rims	117	43.4	2.9
	Crater rims only	12	46	1.8
	ALSEP Pan w/out Crater rims	35	43	2.2
	Near LM w/out Crater rims	35	43.8	2.2
	Near Soil Mechanics Trench, Station 8	13	44.1	2.2
Combinations	Apollo 11,12,14,15 - all data	323	43.8	3
	Apollo 11,12,14,15 - all data w/out Crater rims	273	43.3	2.8
	Apollo 11,12,14,15 - Crater rims only	50	46.7	4
	Apollo 11,14,15 - all data	204	43.7	2.6
	Apollo 11,14,15 - all data w/out Crater rims	185	43.3	2.6
	Apollo 11,14,15 - Crater rims only	19	47.2	2.1
Boulder Tracks	19 Locations on surface	69	43.9	6.6

Table 2-3 – Summary of Porosity Estimates (Heiken et al., 1991)

Basis	Cohesion c (kN/m ²)	Friction Angle φ (deg)	Referenece
Boulder track analysis - Orbiter data	0.35	33	Nordmeyer 1967
Surveyor I strain gage and TV data	0.15 - 15	55	Jaffe 1967
Surveyor I	0.13 - 0.4	30 - 40	Christensen et al. 1967
Surveyor III, soil mechanics surface samples		> 35	Scott and Roberson 1968
Surveyor III, landing data	0 for 10 for	45 - 60 0	Christensen et al. 1968
Surveyor VI, vernier engine firing	> 0.7 for	35	Christensen et al. 1968
Surveyor VI, attitude control jets	0.5 - 1.7		
Surveyor III and VII, soil mechanics surface samples	0.35 - 0.7	35 - 37	Scott and Roberson 1969
Lunar orbiter boulder track records	0.1	10 - 30	Moore 1970
Lunar orbiter boulder track records	0.5	21 - 55	Hoaland and Mitchell 1971

Table 2-4 – Pre-Apollo strength property estimates (Heiken et al., 1991)

Mission	Basis	Cohesion c (kN/m ²)	Friction Angle φ (deg)	Reference
Apollo 11	Astronaut Footprints, LM landing data	Consistent w/ Surveyor		Costes et al. 1969
	Crater slope stability			
Apollo 11	enetrometer tests in LRL on bulk soil samples	0.3 - 1.4	35 - 45	Costes et al. 1970
Apollo 11	Penetration of core tubes, flagpole, SWC shaft	0.8 - 2.1	37 - 45	Costes et al. 1971
Apollo 12	Astronaut Footprints, LM landing data	Consistent w/ Surveyor		Scott et al. 1970
	Crater slope stability			
Apollo 12	Penetration of core tubes, flagpole, SWC shaft	0.6 - 0.8	38 - 44	Costes et al. 1971
Apollo 14	Soil mechanics Trench	< 0.03 - 0.3	35 - 45	Mitchell et al. 1971
Apollo 14	Apollo simple penetrometer	Shear = or > than Surveyor		Mitchell et al. 1971
Apollo 14	MET tracks		37 - 47	Mitchell et al. 1971

Table 2-5 – Apollo strength property estimates (Heiken et al., 1991)

3. ENGINEERING PROPERTIES OF LUNAR SOILS

Chapter 2 summarized the history and procedures involved in lunar soil sampling and testing associated with the Surveyor and Apollo programs. Discussion of sample quality, in-situ and laboratory testing were included, as well as some observational techniques used to determine soil properties. Laboratory testing is an essential element in the characterization of lunar soils. Tests that were run on returned Apollo core samples constitute the bulk of this information. Sieve Analyses were conducted on returned samples in order to assess variation of grain size and distribution with location (Costes and Mitchell, 1970; Scott et al., 1971; Mitchell et al., 1972; Heiken et al., 1991). Vacuum direct shear and vacuum oedometer tests were run in order to obtain strength and deformation parameters respectively (Carrier et al., 1972a). Furthermore, miniature triaxial shear (Jaffe, 1973) and miniature direct shear (Scott, 1987) were also run for obtaining strength parameters. Strength has also been estimated using lab penetration tests (Costes and Mitchell) and trenching tests performed on the lunar surface (Mitchell et al., 1972). This chapter summarizes the information on the physical and engineering properties of the lunar soil, with comparisons to terrestrial soil where applicable.

3.1. PHYSICAL CHARACTERISTICS OF RETURNED LUNAR SOILS

Although the composition the returned lunar soils varied slightly from site to site, geotechnical engineers have quoted the same general classification. The soils are described as a brownish to medium gray, slightly cohesive granular soil in the silt to fine sand range (Costes and Mitchell, 1970). The soils are well graded, with a wide range of particle sizes. Grain size distributions for lunar soils are typically the same for particle sizes greater than 1 mm. For the purposes of geotechnical testing and analysis, the component with particle size less than 1mm is usually quoted. Figure 3-1 shows the typical grain size distribution curves for the Apollo 11 samples. Figure 3-2 shows the similarity between in particle size distribution between samples obtained on four Apollo missions. A few cases of coarser grained material have been found in bands within lunar core tubes and at the bottom of trenches. These grain size distributions fall outside of the range for typical lunar soils (Figure 3-2). The distributions are similar to those of terrestrial well-graded silty sand to sandy silt, SW-SM to ML in the Unified Soil Classification System (Heiken et al., 1991).

Particle size, shape and angularity are also important properties that have direct effect on strength in granular materials. The angularity of a soil particle is typically measured by its ratio of the average radii at the corners of the particle (estimated from photographic images) to its maximum inscribed circle. Particle angularity can be divided into four categories: Angular, Subangular, Subrounded and Rounded (Das, 1998). Lunar soils fall into the angular to subangular range, with angularity values of 0.19 to 0.26 (Heiken et

al., 1991). Figure 3-3 shows some angular terrestrial sand particles, similar in shape to lunar soils. Chapter 2 briefly discussed agglutinates and breccia materials, particles of which tend to be angular and have rough textures.

Specific gravity measurements were conducted using a variety of methods, the most common being water or gas pycnometry. Pycnometry is the process by which particles are placed into a fluid and measurements are made of the volume displaced. Measurements of specific gravity are dependent on the amount of subgranular voids that exist in the particles. These voids exist inside the particle grains (e.g. hollow glass sphericals). Therefore, soils with a high number of subgranular voids will be measured having a higher specific gravity than in reality. However, the extent of these voids is still poorly understood. Actual specific gravity measurements are extremely sensitive to the composition of the soil at a particular site. A summary of various tests can be seen in Table 3-1. Gas pycnometers are also used in conventional terrestrial laboratories. The standard soil mass for the test, as outlined in ASTM D854, is 100g (www.astm.org). Testing conducted on lunar samples had a maximum sample size of 57 grams, Table 3-1. Sample size is sure to effect the values produced from these tests.

Table 3-1 summarizes measurements of specific gravity from returned Apollo samples that show varying G values over a wide range, 2.9 to 3.5. At the lower end of this range are samples possibly containing a higher percentage of hollow glass particles, while basaltic minerals generally raise the measured values. The average specific gravity that is widely quoted, $G = 3.1$, is significantly higher than the average value quoted (2.7) for terrestrial soils.

This difference can be directly attributed to the geological processes (volcanic activity, bombardment by large projectiles).

One of the most important parameters associated with lunar soils is the bulk density, ρ , defined as the mass of material per unit volume.² Bulk density measurements have been made with direct and indirect methods. Direct measurements can be made using core tube samples. However, disturbance (i.e. volume changes during insertion and core retrieval) can play a large part in the accuracy of the data from this method. As discussed in Chapter 2, the tubes from Apollo 15 and on are the least disturbed, and will therefore yield the best data. Table 3-2 summarizes the various tests and results.

Early estimates of in-situ density were extremely poor. Observations of the lunar surface using remote photographs from Ranger probes yielded estimates of porosity, $\rho = 0.3 - 0.4 \text{ g/cm}^3$. A value of $\rho = 0.3 \text{ g/cm}^3$, based on $G = 3.1$, corresponds to a void ratio, $e = 9$ (Mitchell et al., 1972a).³ Terrestrial values of density fall close to those observed on moon. However, the formational mechanisms that led to the deposition of the materials are very different. The lunar surface is devoid of weather, water and life, three important factors affecting the distribution and packing of soils on earth.

Best estimates for the in-situ density based on the data in Table 3-2 are shown in Table 3-3 (Heiken et al., 1991).

$$^2 \rho = \frac{\gamma_t}{g} = \left(\frac{G}{1+e} \right) \left(\frac{\gamma_w}{g} \right)$$

$$^3 e = \frac{n}{(1-n)}$$

It should be noted that a major controlling factor is the lunar gravity, $\mathbf{g_L} = 0.167 \mathbf{g_E}$, where $\mathbf{g_E}$ is the earth's gravitational acceleration ($\mathbf{g_E} = 9.81 \text{ ms}^{-2}$). Therefore, it can be deduced that under lunar conditions, the ultimate bearing capacity is highly dependent on the cohesion. However, under earth's gravitational conditions, the magnitude of cohesion is small compared to frictional effects. The cohesive properties of lunar soil seem small in earth conditions, but their significance in lunar gravity may be more notable.

It is common geotechnical practice to characterize the engineering properties of granular soil through relative density, $\mathbf{D_r}$.

$$D_r = \frac{(e_{\max} - e)}{(e_{\max} - e_{\min})} \times 100(\%)$$

where $\mathbf{e_{\max}}$ and $\mathbf{e_{\min}}$ are minimum and maximum void ratios obtained by preparing samples according to methods defined by ASTM D-2049 (www.astm.org). Maximum void ratio is calculated by pouring sand loosely through a funnel with a 1/2" diameter spout into a mold with a volume of 0.1 ft³. Minimum void ratio is calculated by vibrating sand in a mold for a period of 8 minutes, with a surcharge of 2 psi on top (Das, 1998). These values are very useful for comparing properties of soil from different geological origins. Values of $\mathbf{e_{\max}}$ and $\mathbf{e_{\min}}$ calculated for Apollo core samples are summarized in Table 3-4. The relationships between relative density and porosity/void ratio are shown in Figure 3-4.

The usefulness of relative density measurements on lunar soils is still unclear. However, it does give engineers and scientists a basis of comparison with terrestrial soils.

3.2. SHEAR STRENGTH PARAMETERS

Shear strength properties of lunar soil affected the bearing capacity (stability) of the lunar module footing pads, as well as the penetration resistance of sampling tools, embedment of the lunar rover and the astronaut's ease of movement. Reliable estimates of strength parameters are also critical for proposed designs of constructed facilities the moon. To date, the interpretation of strength parameters for lunar soils has focused exclusively on the Mohr-Coulomb criterion for cohesive-frictional material with input parameters c and ϕ , respectively. The M-C criterion defines a linear failure envelope in the shear-normal stress space, Figure 3-5.

It is not surprising that lunar soil is frictional, given the descriptions of particles from early photographs and explorations. The sources of the cohesive strength are much less clear. The cohesion of lunar soil was measured indirectly as far back as the Surveyor program. Estimates of cohesion were made from Surveyor I photography alone (Surveyor I was not equipped with the testing arm). The response of the Surveyor lander's footpads and observations of the surrounding area were the primary basis for these estimates. A range of cohesion values, $c = 0.02$ to 0.05 psi (0.15 to 0.35 kPa), was chosen (Christensen et al., 1967). It is important to note that the exact value of these estimates is not as important as is the fact that lunar soil possesses a measurable cohesion.

The cohesive component of strength has been investigated by a series of trenching experiments carried out as part of the Apollo 14 and 15 missions. According to plasticity theory, the stability of a trench of depth in homogeneous soil, H , and inclination, B (Figure 3-6), is a function of the friction angle and the cohesion. By measuring the failure heights for different values of B , it is possible to infer the values of c and ϕ . For example, for a cohesion, $c = 0.35$ kPa, a friction angle, $\phi = 35^\circ$ and density, $\rho = 1.9$ g/cm³, a vertical cut of 85 cm would be possible before failure (Mitchell et al., 1972). Estimates of lunar soil cohesion were also made using trenching tests conducted on the Apollo missions. Values of cohesion from the Apollo 14 and 15 trenching tests ranged from $c = 0.03$ to 1.0 kPa.

Scott et al. (1971) attributed this cohesion to electrostatic attraction forces generated by the bombardment of lunar soils by the solar wind.

Many methods were used to estimate the failure parameters ϕ and c . The parameters can be backfigured using measurements from the penetration measurements obtained using the Apollo Simple Penetrometer (ASP), also used on the Apollo 14 mission. Unfortunately, penetration resistance is also affected by the compressibility of soil and, therefore, there is uncertainty in backfigured values of ϕ and c from penetration resistance measurements. In Mitchell et al. (1972b), interpretations of ϕ and c were made using a conventional bearing capacity equation:

$$\frac{F}{A} = cN_c + \rho gzN_q$$

where **F** is the measure resistance, **A**, the cross-sectional area of the penetrometer and **N_c** and **N_q** bearing capacity factors.

More reliable penetration data were obtained in Apollo 15 and 16 missions using the Self-Recording Penetrometer (SRP). Penetration resistance vs. depth for the Apollo 16 SRP tests is plotted in Figure 3-7. Values of cohesion and friction angle estimated from the SRP measurements of Apollo 15 and 16 can be seen in Table 3-5.

Comparisons of strength parameters from penetration and trenching tests for Apollo 15 are shown in Figure 3-8. The results shown are the parameters for incipient failure the trench wall and for the application of a 25-lb force on the SRP and varying depths. The trench tests results show a cohesion that is almost independent of friction angle, while the penetration results show a strong relation between friction angle and cohesion. Further investigation is necessary to refine this relationship.

Laboratory tests conducted on returned lunar soil samples are the most direct method for obtaining strength parameters, but are also prone to disturbance effects from sampling operations and transportation. Laboratory tests on returned lunar soil included 12 laboratory penetrations on Apollo 11 samples (Costes and Mitchell, 1970), 3 vacuum direct shear tests (Jaffe, 1973),

5 series of miniature direct shear tests (Carrier et al., 1972a), and 2 miniature triaxial tests (Scott, 1987) on Apollo 12 samples.

The laboratory penetration tests were conducted with the use of a small spring-loaded pocket penetrometer, Figure 3-9. Table 3-6 summarizes the results from these tests. In some cases the penetration did not meet with enough resistance to compress the spring. In these cases, the weight of the penetrometer was taken 1.8 N (Costes and Mitchell, 1970).

Vacuum tests were designed to eliminate the potential problems associated with particle contamination. Humidity present in the terrestrial atmosphere was seen as a potential source for error in the laboratory tests. In fact, Scott (1973) observed that exposure to earth air caused the Specific Surface Area (SSA) of lunar soil particles to double from $SSA = 0.5 \text{ m}^2/\text{g}$ to $1.0 \text{ m}^2/\text{g}$.⁴ The implications of entrapped water on the surface of lunar soils are that, having lost their initial properties upon exposure, they may behave more like terrestrial soils with a small water content. Three vacuum direct shear tests were run on using 200 grams of returned Apollo 12 samples. For complete contamination protection, the samples were also prepared in a vacuum. Table 3-7 shows the results of these tests.

Due to the small quantities of soil available, miniature versions of the direct shear and triaxial cell had to be made. The miniature triaxial (Figure 3-10) cell tested samples that were 6mm in diameter and 12mm high. The sample mass for these tests was approximately 0.9 gm for lunar soil. In contrast, in a conventional triaxial cell uses samples that are 36 mm in

⁴ SSA is a measurement of a soil particle's surface area per unit mass.

diameter and 76 mm high. The volume ratio of typical to miniature sample size is about 224:1. The small size of the testing apparatus and the effect it has on the quality of the results is an important point affecting measured parameters. A series of tests were run with the mini-triaxial cell on a fine grained terrestrial soil composed of crushed Leighton Buzzard sand, in order to check the accuracy of the data obtained. It was found (Scott, 1973), that the size of the apparatus had no effect on strength property measurements. Results of the mini-triaxial tests are shown in Table 3-8.

The miniature direct shear tests were conducted the returned lunar soil from Apollo 12 taken from the Surveyor 3 scoop. These tests constitute a large amount of the laboratory strength data. The results from these tests are shown on Figure 3-11 and tabulated in Table 3-9. The high failure envelope for Series 5 is unexplained.

Considerations of test procedures and conditions are important when evaluating the given strength data. Factors possibly contributing to error in these results include sample size and high stress conditions. In fact, the confining stresses applied to the test samples were usually one to two orders of magnitude higher than seen on the Moon (Heiken et al., 1991). Scott (1973) states:

It must be expected that some of its [lunar soil] mechanical properties in terrestrial tests would be different from those of the same material on the moon, because of the extreme environmental change the material has undergone even in its best-preserved state.

Furthermore, because of the re-use of samples from one test run to another, particle breakdown may be a large additional source of error.

Several studies by Carrier et al. (1972, 1973), Mitchell et al. (1974) and Leonovich et al. (1974) suggest that a curved Mohr-Coulomb equation would better describe the strength of lunar soils. It has been suggested that the following relationships be used (Heiken et al., 1991).

$$\tau = a \sigma^b$$

$$\phi = \tan^{-1} (ab \sigma^{b-1})$$

$$c = a (1-b) \sigma^b$$

Carrier (1972, 1973) has suggested using values of $a = 1.83$ and $b = 0.73$ (Heiken et al 1991). Stresses are in kPa. A plot of the curved envelope compared with a conventional envelope can be seen in Figure 3-12.

Compiled strength relationships for Surveyor, Apollo and Russian Lunokhod missions are shown in Figure 3-13. The results are shown bounded by results of tests on basaltic lunar soil simulants at different relative densities.

Recommended values of strength parameters (Heiken et al., 1991) c and ϕ are shown in Table 3-10.

3.3. DEFORMATION PROPERTIES

Elastic stiffness properties derived from geophysical measurements of shear/compression wave velocity profiles provide the only direct data for inferring the deformation properties of in-situ lunar soils. Geophysical measurements were carried out on Apollo 14 and 16 through the Active Seismic Experiment. The methods used were very similar to terrestrial geophysical seismic reflection techniques. A device called the “Thumper” generated elastic compression waves. The thumper comprised a short staff used to detonate small explosive charges. It was capable of holding up to 21 explosive charges that were mounted to a base plate at the bottom. Elastic waves were also generated using a mortar assembly, capable of launching shells to distances of 900 m (Apollo 16 only). Arrival times of the waves were measured by a series of geophones, miniature moving coil-magnet seismometers, placed 45 meters apart in a line along the ground surface. The wiring on the geophones was connected to a three-channel amplifier, for telemetering the data back to earth. The frequency range of the geophones was 3 to 250 Hz. The predicted maximum depth of the experiment was about 460 m. The device measured two P-wave velocities near the Fra Mauro site (Apollo 14). Close to the surface, P-wave velocities were 104 m/s. At a depth of 8.5 meters, the velocity was approximately 300 m/s. Furthermore, velocities of this magnitude (0.1 to 0.3 km/s) were seen in the upper few hundred meters at all test sites. These velocities are much lower than observed for intact terrestrial rock. Therefore, it is assumed that the higher end of the values corresponds to highly fractured/brecciated material.

Measurements of P-wave velocities can be used to calculate the elastic shear modulus at small strains, \mathbf{G}_{\max} , of a material, which in turn can be used to obtain values of Young's Modulus, \mathbf{E}_{\max} .⁵ P-wave velocity, \mathbf{v}_p is related to shear wave velocity, \mathbf{v}_s , by the following relationship:

$$\nu = \frac{v_s^2 - 0.5v_p^2}{v_s^2 - v_p^2}$$

where ν = Elastic Poisson's Ratio.

Elastic shear modulus, \mathbf{G} , is related to \mathbf{v}_s by:

$$G = (\rho V_s)^2$$

where ρ = density.

Assuming a value of Poisson's ratio, P-wave velocities can be used to calculate values for \mathbf{G}_{\max} and \mathbf{E}_{\max} . The elastic shear modulus can also be estimated an empirical correlation generated by Hardin and Black (1966) for terrestrial soils:

$$G = 3228 \frac{(2.973 - e)^2}{(1 + e)} \sigma^{0.5}$$

⁵ $G = \frac{E}{(1 + \nu)}$

where e is the void ratio and σ is the average effective stress (in kPa) on the soil. Data from the vacuum oedometer tests conducted by Carrier et al. (1972a) were used in the Hardin and Black equation. The data from the seismic experiments and the estimations made by the Hardin and Black equation are shown in Figure 3-14.

The Hardin Black equation and the results of the seismic experiments are in poor agreement at shallow depths (less than 8.5m). However, at depths greater than 8.5m, the approximation and the recorded data correlate much better.

For purposes of calculating settlement, compressibility and stiffness properties are also important. Typically, the parameters of engineering interest are the average elastic modulus, E , and compressibility parameters C_c and C_r . As previously discussed, shear wave velocity measurements using surface geophysical techniques can be used for estimates of E . Carrier et al. (1972a) discuss the estimation of compressibility parameters using vacuum oedometer tests. The following paragraphs will describe the methods and results of these tests.

Vacuum oedometer tests were used for observing the compressive behavior of lunar soils and measuring its corresponding parameters. These tests that were run in conjunction with the vacuum direct shear test discussed previously, in which the compressive data was recorded during the consolidation phase. These parameters are defined as the slopes of the compression and recompression curves on a plot of e vs. $\log \sigma_v$ produced during a 1-D compression test. The results of the two vacuum oedometer tests are

shown in Figure 3-15. Recommended values (Heiken et al., 1991) of C_c and C_r for lunar soils are shown in Table 3-11.

The compressibility of the loose soil deposits is high. Considerations for settlements of lunar structures will rely heavily on the values and variations throughout a proposed site. Further data concerning compressibility of lunar soils would be useful for these purposes.

The vacuum oedometer also produced some interesting and perhaps useful results. The compression of the lunar soil produced levels of Hydrogen and Helium gas in the vacuum chamber. These gases are thought to be trapped inside volcanic sphere and agglutinate particles. Once the applied stress is high enough, the particles crush and the gas is released. It has been theorized that gas is released upon exceeding the soil's maximum past pressure. If so, this would be a useful property to help better understand lunar soil history (Carrier et al., 1972a).

FIGURES

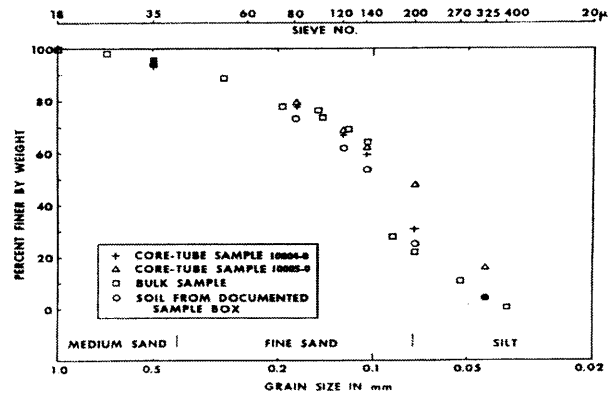


Figure 3-1 - Apollo 11 Grain Size Curve (Costes and Mitchell, 1970)

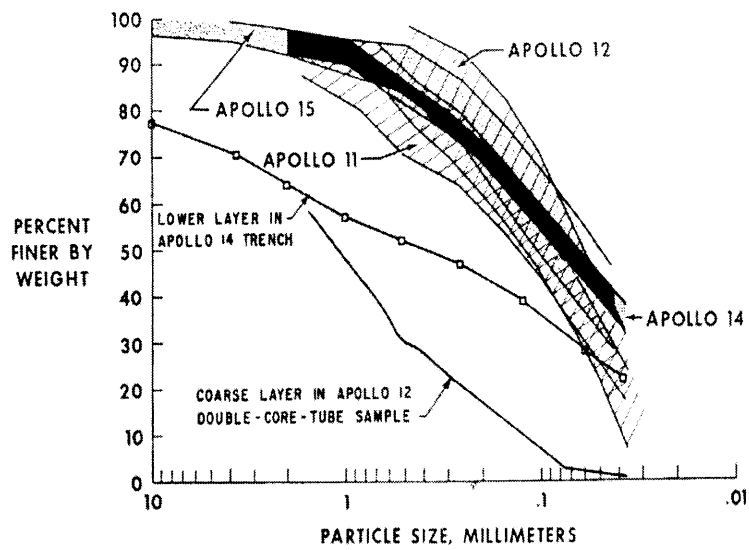


Figure 3-2 - Grain Size Curves for Apollo 11, 12, 13 and 14 Soils. (Mitchell et al., 1972a)

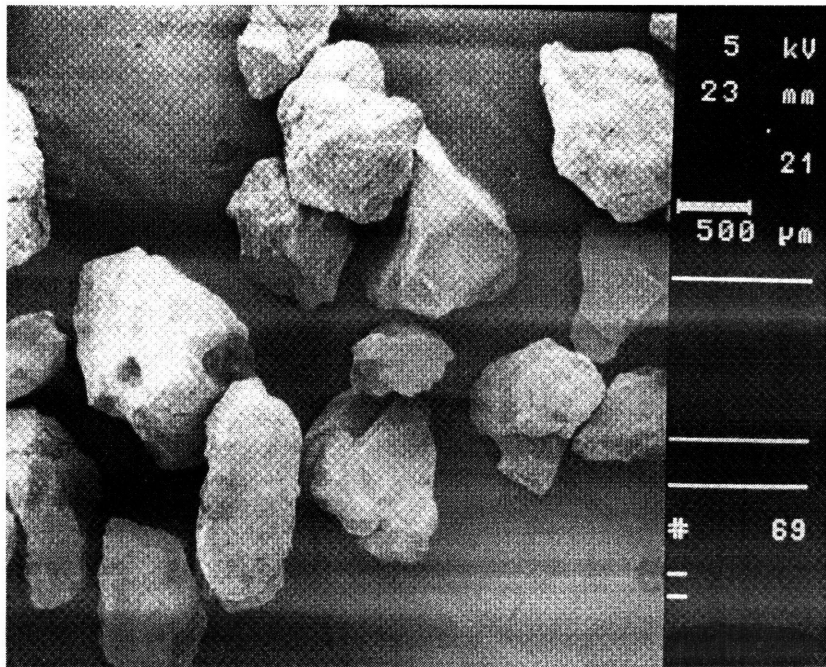


Figure 3-3 – Angular terrestrial sand. (Das, 1998)

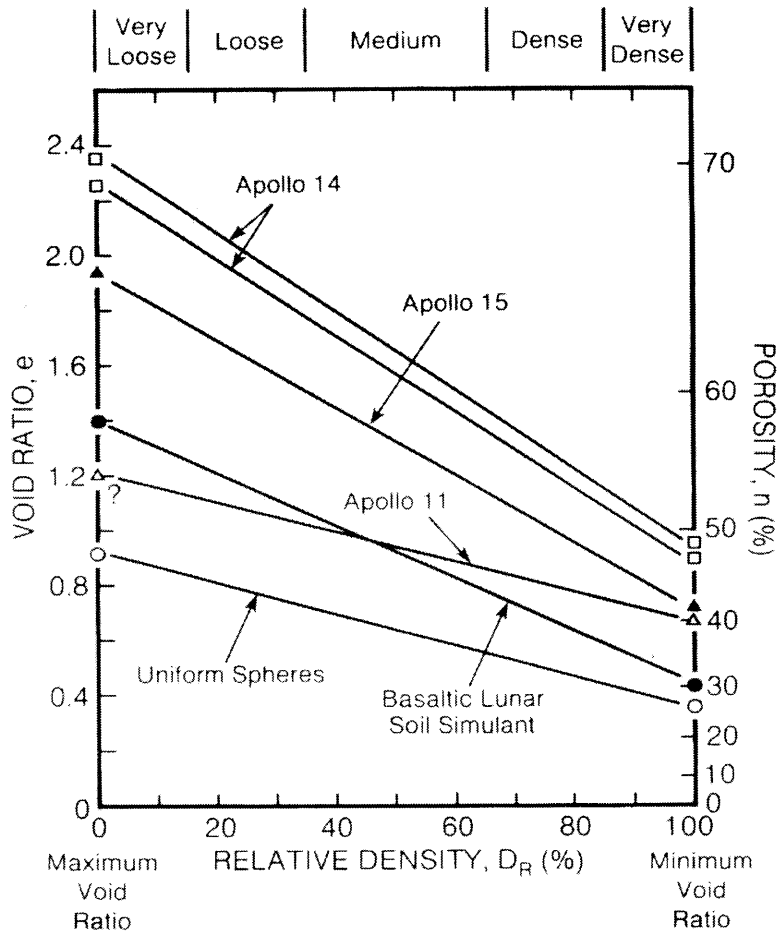


Figure 3-4 – Relationship between porosity/void ratio, Relative Density and depth for Apollo soil samples, a basaltic lunar simulant and the ideal case of uniform spherical particles (Heiken et al., 1991).

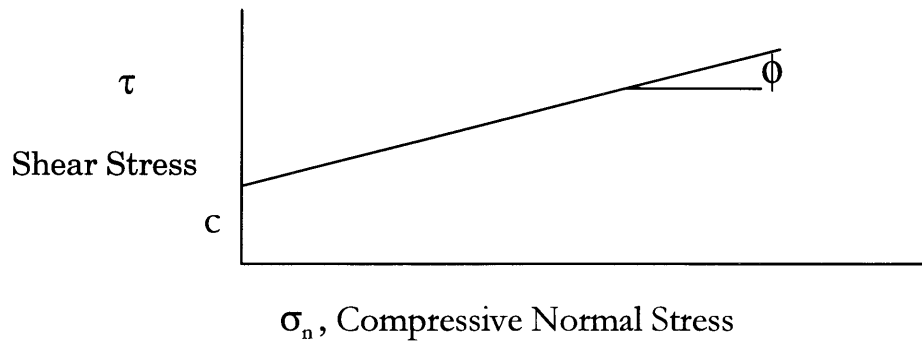


Figure 3-5 Mohr-Coulomb strength envelope for cohesive-frictional materials.

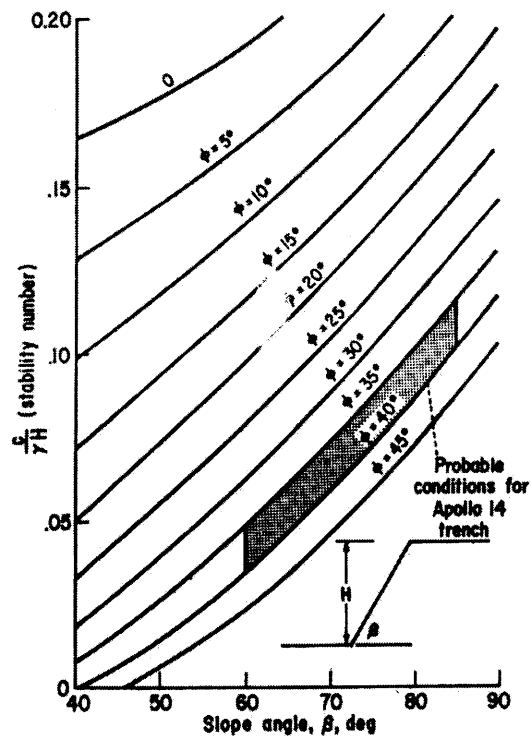


Figure 3-6 - Stability Numbers for Lunar Slopes. (Mitchell et al., 1972)

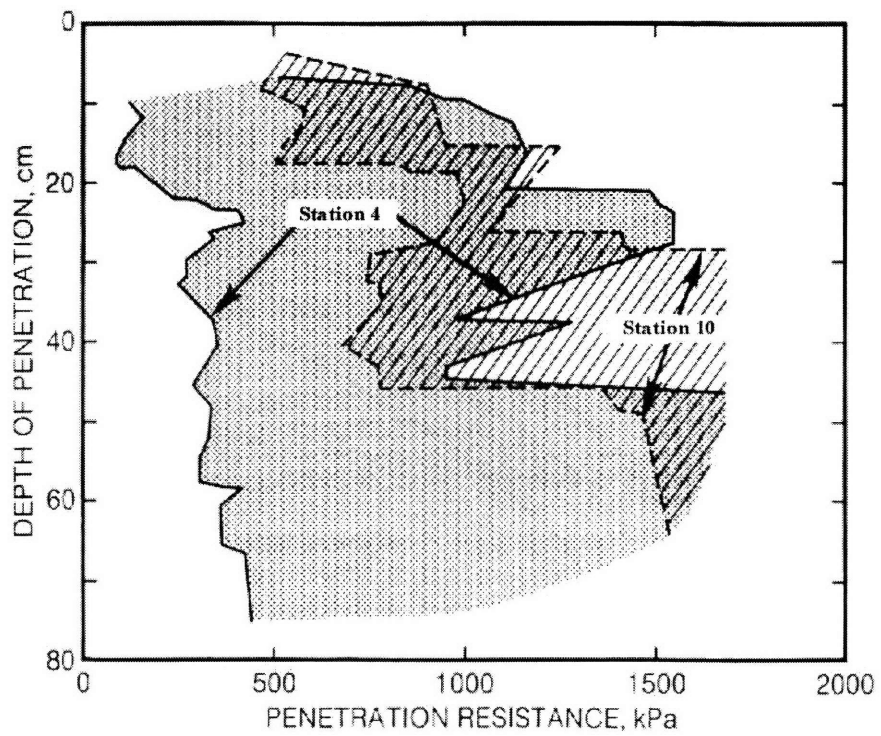


Figure 3-7 - Penetration resistance vs. depth for the Apollo 16 SRP at two locations. (Heiken et al., 1991)

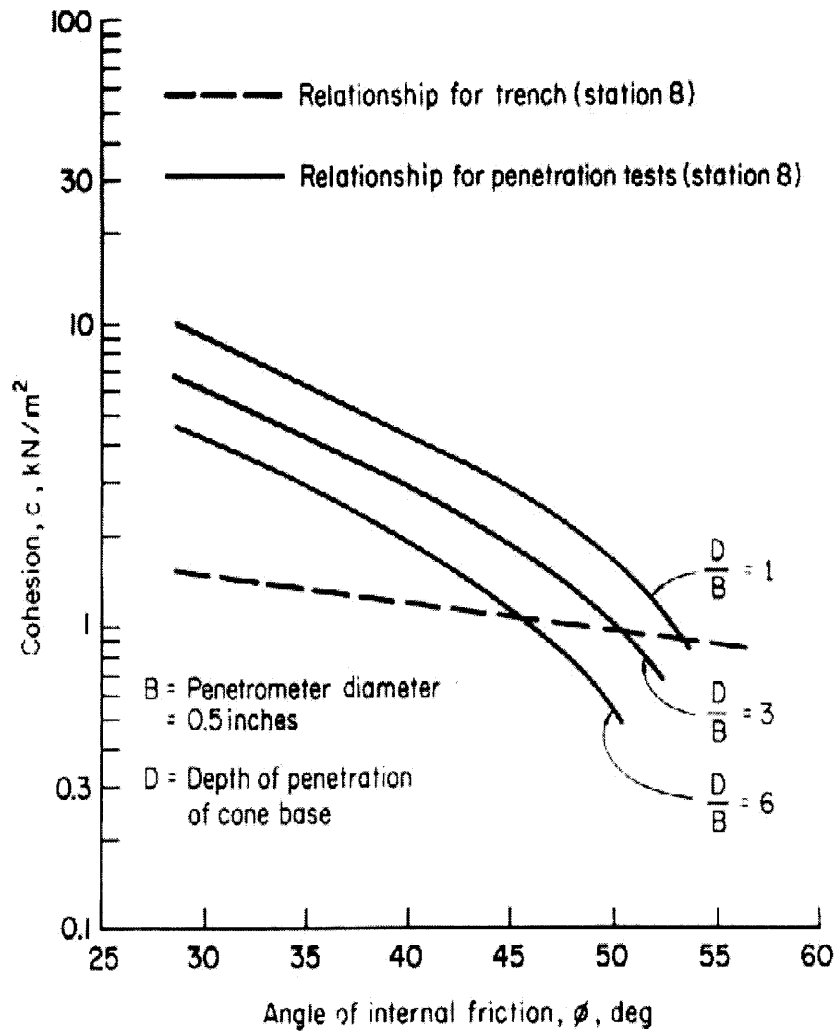


Figure 3-8 – Comparison of strength parameter variations for Apollo 15 trench and penetration tests. (Mitchell et al., 1972a)

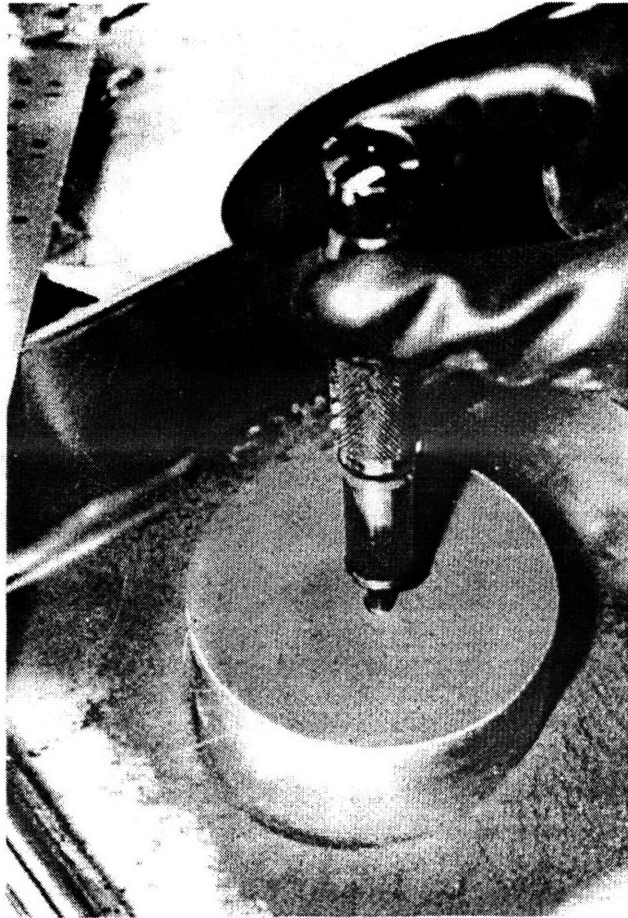


Figure 3-9 – Laboratory penetration test.
(Costes and Mitchell, 1970)

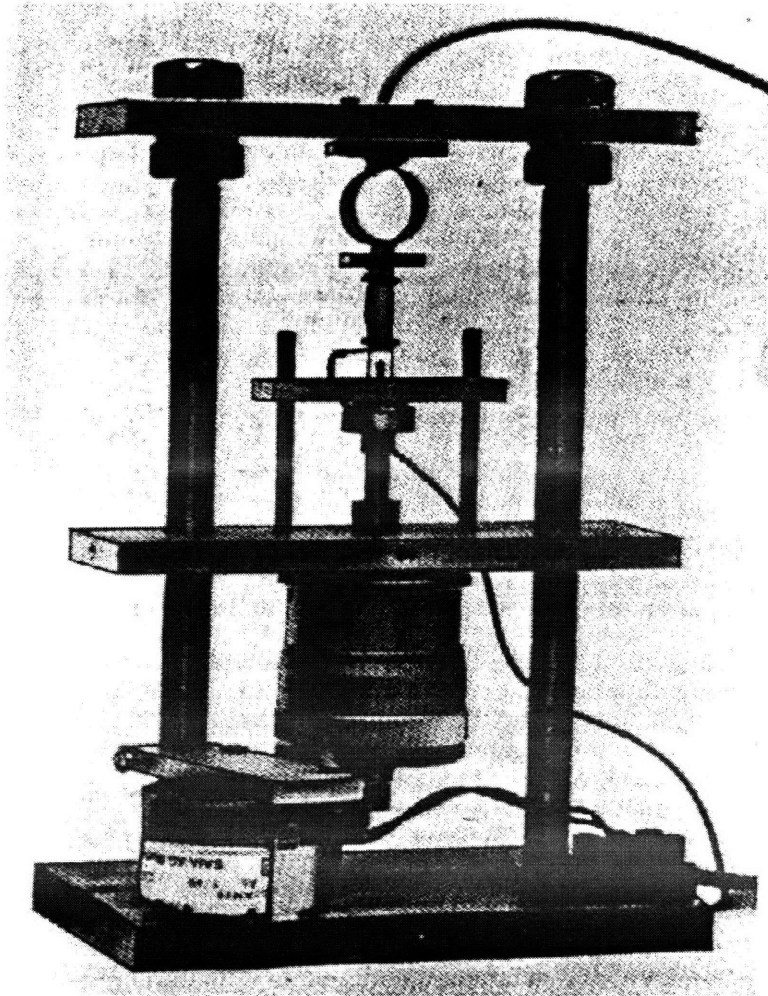


Figure 3-10 – Miniature Triaxial testing apparatus. (Scott, 1973)

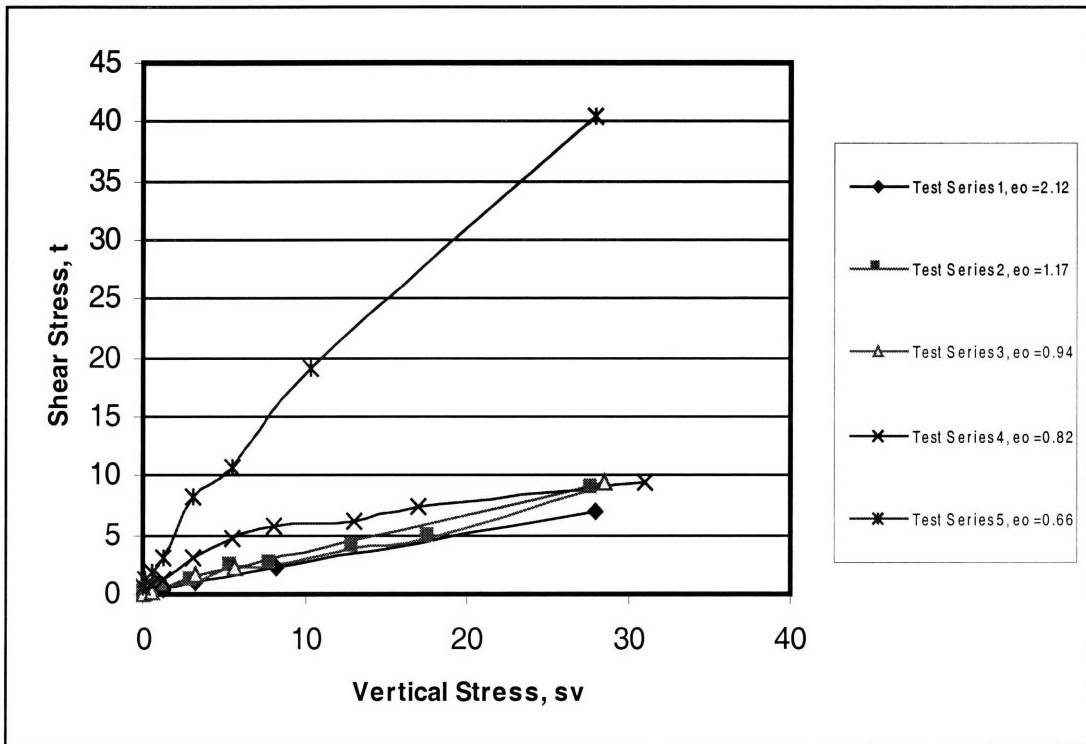


Figure 3-11 – Failure Envelopes of Miniature Direct Shear tests. All tests were run on returned soil from the Surveyor 3 scoop (Apollo 12). Stresses in kPa. (Heiken et al., 1991)

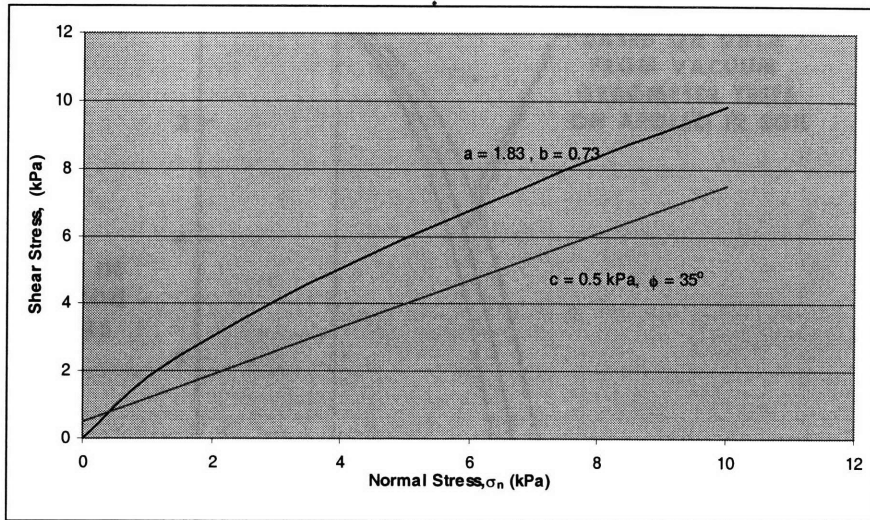


Figure 3-12 – Comparison of proposed curved strength relationship with conventional envelope. Chosen cohesion and friction angle from a range of values described by lunar trench tests.

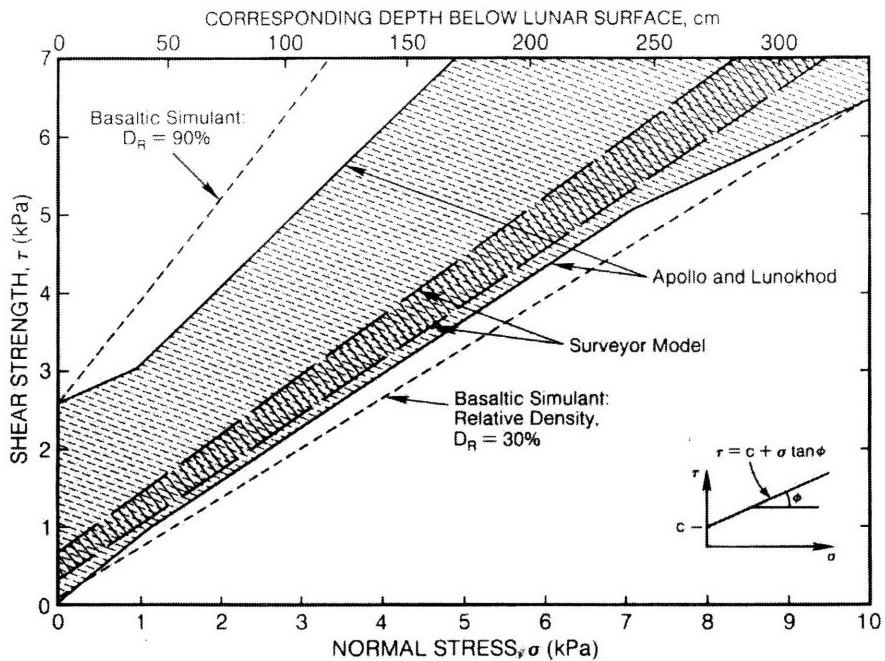


Figure 3-13 - Shear Strength vs. Normal Stress for lunar soil and basaltic lunar simulants (Heiken et al., 1991).

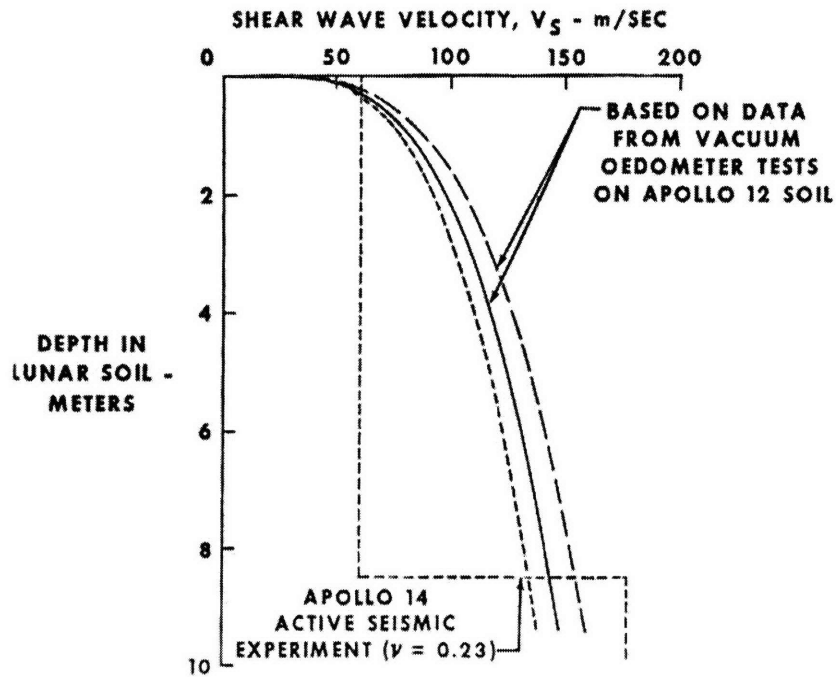


Figure 3-14 – Shear wave velocity vs. depth relationships from the Apollo 14 Active Seismic Experiment and the Hardin-Black equation applied to vacuum oedometer data (Carrier et al., 1972).

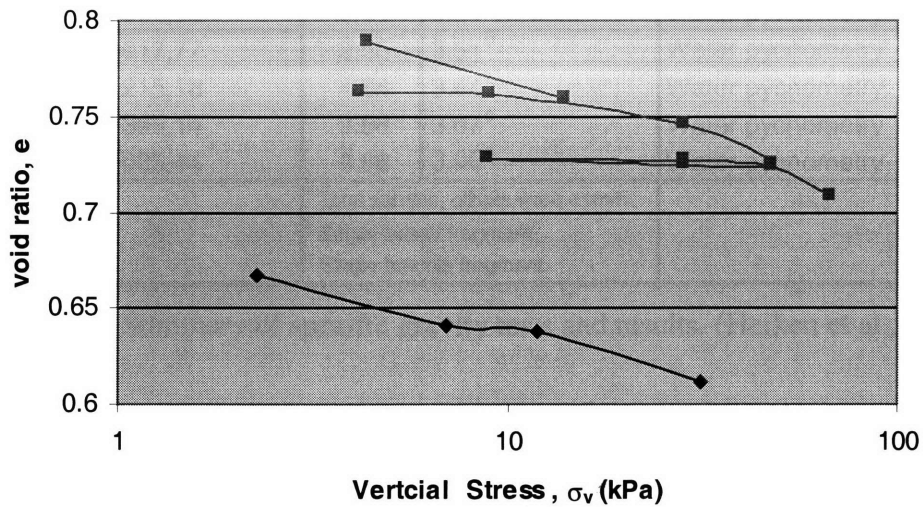


Figure 3-15 - Results of 2 vacuum Oedometer tests. Stress in kPa. (Heiken et al., 1991)

TABLES

Mission	Sample Number	Sample Weight (grams)	Specific Gravity G	Test Technique
Apollo 11	10004 & 10005	49.1	3.1 ^a	Nitrogen pycnometry
	10020,44	5.94	3.25 ^b	Water pycnometry
	10065,23	4.48	3.12 ^c	Suspension in Density Gradient
Apollo 12	Apollo 12 (no #)	1.5	3.01	Air pycnometry
	12002,85	56.9	3.1 ^a	Water pycnometry
	12029,8	2.32	2.9	Nitrogen pycnometry
	12057,72		2.9	Unknown
Apollo 14	14163,111	1.1	2.9 +/- 0.1	Helium pycnometry
	14163,148	0.65	2.9 +/- 0.05	Water pycnometry
	14259,3	0.97	2.93 +/- 0.05	Water pycnometry
	14321,74	1.26	3.2 +/- 0.1 ^c	Helium pycnometry
	14321,156		3.2 +/- 0.1 ^c	Helium pycnometry
Apollo 15	15015,29		3.0 +/- 0.1 ^c	Helium pycnometry
	15101,68		3.1 +/- 0.1	Helium pycnometry
	15601,82	0.96	3.24 +/- 0.05	Water pycnometry
Apollo 17	70017,77	2.55	3.51 ^b	Water pycnometry
	70215,18	4.84	3.44 ^b	Water pycnometry
	72395,14	3.66	3.07 ^c	Water pycnometry
	77035,44	3.68	3.05 ^c	Water pycnometry
		^a Total sample, others were <1mm		
		^b Single basalt fragment.		
		^c Single breccia fragment.		

Table 3-1 – Summary of specific gravity tests and results. (Heiken et al., 1991)

Mission	Returned Core	Bulk Density (g/cm ³)	Reference
Apollo 11		1.54 - 1.75	Costes and Mitchell 1970
		0.75 - 1.75	Scott et al. 1971
Apollo 12		1.6 - 2.0	Scott et al. 1972
		1.55 - 1.90	Houston and Mitchell 1971
		1.7 - 1.9	Carrier et al. 1971
Apollo 14		1.45 - 1.6	Carrier et al 1972
Apollo 15	Core Tubes	1.36 - 1.85	Carrier et al 1972, Mitchell et al. 1972
	Drill Cores	1.62 - 1.93	Carrier 1974, Mitchell et al. 1972
Apollo 16	Core Tubes	1.4 - 1.8	Mitchell et al. 1972
	Drill Cores	1.47 - 1.75	Carrier 1974
Apollo 17	Core Tubes	1.57 - 2.29	Mitchell et al. 1974
	Drill Cores	1.74 - 1.99	Carrier 1974

Table 3-2 – Summary of mass density measurements from Apollo core samples (Heiken et al., 1991).

Depth (cm)	Density (g/cm ³)
0 - 15	1.45 – 1.55
0 - 30	1.52 – 1.63
30 - 60	1.69 – 1.79
0 - 60	1.61 – 1.71

Table 3-3 – Estimates of lunar soil density vs. depth. (Heiken et al., 1991)

Mission	Sample Number	Sample Weight	Density (g/cm ³)		Specific Gravity G	Void Ratio		References
			ρ_{min}	ρ_{max}		e_{min}	e_{max}	
Apollo 11	10084	565	1.36	1.80	3.01	1.21	0.67	Costes et al. 1970
	10084,68	5	1.26		3.01	1.39		Cremers et al. 1970
Apollo 12	12001, 19	6	1.30					Cremers and Birkebak 1971
	12029, 3	6.5	1.15	1.93				Jaffe 1971
Apollo 14	14163,133	5	1.10		2.9±0.1	1.64		Cremers 1972
	14163,148	0.97	0.89±0.03	1.55±0.03	2.90±0.05	2.26	0.87	Carrier et al. 1973
	14259,3	1.26	0.87±0.03	1.51±0.03	2.93±0.05	2.37	0.94	Carrier et al. 1973
Apollo 15	15031,38	5	<1.30					Cremers and Hsia 1973
	15601,82	0.96	1.10±0.03	1.89±0.03	3.24±0.05	1.94	0.71	Carrier et al. 1973

Table 3-4 – Measured minimum and maximum densities of lunar soils from Apollo samples. (Heiken et al., 1991)

Source	Cohesion, c (kPa)	Friction Angle ϕ ($^{\circ}$)
Apollo 15	1	47.5 - 51.5
Apollo 16		
Station 4	0.6	46.5
Station 10	0.37	49.5
Station 10	0.25 - 0.60	50-47

Table 3-5 – Summary of strength parameters from SRP tests. (Heiken et al., 1991)

Test	Density (g/cm ³)	Force (N)	Area (cm ²)	Pressure (N/cm ²)	Penetration cm	Pressure/Penetration Ratio (N/cm ² per cm)
1	1.36	<1.8	0.316	<5.7	0.64	
2	1.36	<1.8	0.316	<5.7	1.96	
3	1.36	<1.8	0.316	<5.7	1.96	
4	1.36	<1.8	0.316	<5.7	1.96	
5	1.36	3.1	2.68	1.14	2.01	0.57
6	1.72	1.8	0.316	5.7	0.81	7.03
7	1.72	5.1	0.316	17.1	1.7	10.2
8	1.72	<1.8	0.316	<5.7	0.64	
9	1.72	9.8	0.316	30.8	2.54	12.1
10	1.72	5.8	0.316	18.3	2.11	8.66
11	1.72	38.7	2.68	14.3	1.7	8.39
12a	1.8	28.9	2.68	10.8	0.66	16.5
12b	1.8	79.8	2.68	29.7	1.96	22.9

Table 3-6 – Summary of laboratory penetration tests on returned Apollo 11 sample. (Costes and Mitchell, 1970)

Test Number	Void Ratio e	Vertical Stress σ_v (kPa)	Peak Shear Stress τ (kPa)	τ/σ_v	Friction angle ϕ
1	0.612	31.21	21.22	0.68	34
1B	0.55	69.92	50.15	0.72	35
2	0.708	67.51	36.3	0.54	28

Table 3-7 – Results of Vacuum Direct Shear tests. Values of c = 0 to 0.7 kPa. (Carrier et al., 1972)

Mini-Triaxial Test ^a				
Void Ratio e	Confining Stress σ_3 (kPa)	Peak Shear Stress τ (kPa)	Axial Strain at Peak Shear (%)	Friction Angle ϕ
0.69	26	157	5.3	59
0.87	52-55	192	8.9	51-52

Table 3-8 – Results of Miniature Triaxial tests. ^a for cohesion $c = 0$ to 1 kPa. (Heiken et al., 1991)

Test Series	Initial Void Ratio	Cohesion, c (kPa)	Friction Angle, ϕ (deg)
1	2.12	0.3	13
2	1.17	0.1	17
3	0.94	0.5	19
4	0.82	3.1	14
5	0.66	2.8	56

Table 3-9 – Results of Miniature Direct Shear Tests. Void ratio was calculated assuming $G = 3.1$. (Heiken et al., 1991)

Depth Range (cm)	Cohesion, c (kPa)		Friction Angle, ϕ (deg)	
	Average	Range	Average	Range
0 - 15	0.52	0.44 - 0.62	42	41 - 43
0 - 30	0.9	0.74 - 1.1	46	44 - 47
30 - 60	3	2.4 - 3.8	54	52 - 55
0 - 60	1.6	1.3 - 1.9	49	48 - 51

Table 3-10 – Recommended values of strength parameters for specific depth ranges. (Heiken et al., 1991)

Compression Parameter	Value	
Cc	Loose Soil	0.3
	Dense Soil	0.05
Cr	0.003	

Table 3-11 – Recommended values of C_c and C_r . (Heiken et al., 1991)

4. EXPERIENCE WITH LUNAR SOIL SIMULANTS

The design of lunar tools, instruments, space vehicles and landing modules all involve geotechnical engineering considerations. As far back as the Surveyor program, lunar soil simulants were used to assist in the design of the surface scoop and testing equipment (Figure 2-21). This chapter reviews the physical properties considered most important in the selection of suitable materials and illustrates the applications of lunar soil simulants in engineering studies.

4.1. SELECTION OF SIMULANTS

The value of simulant testing for lunar soil studies is easy to appreciate given the special circumstances involved in lunar exploration. Lunar soil samples are very difficult to retrieve or test in-situ. Furthermore, large amounts of material are needed in order to calibrate in-situ testing devices, such as the Apollo penetrometers or core samplers. Therefore, the physical properties of the simulants must be selected to provide the closest possible match to behavior of lunar soil in-situ.

Various granular materials have been used as lunar simulants. In order to account for the high specific gravity of lunar soils (average $G = 3.1$), ground

basalts are frequently the source material. Lunar rover studies were conducted prior to Apollo 11 and used a wind blown sand from Yuma, Arizona (Costes et al., 1971). However, much closer matching of properties with real soils only occurred after the return of samples from Apollo 11 and 12. NASA had plans to include more advanced equipment in future Apollo missions. This equipment, which included new testing equipment and vehicles, needed to be studied thoroughly to determine their effectiveness on the lunar surface. Crushed basalt, with a specific gravity of 2.89 was a large component of the simulants used in these early studies.

Figure 4-1 compares the grain size distributions of Apollo 11 and 12 samples with a series of lunar simulants including 1) LSS (40/60 MIX), 2) LSS (11/12 MIX), 3) LSS (WES MIX), 4) Yuma Sand. While a perfect match is not essential, similar grain size distribution curves were considered one of the most important factors in the choice of early simulants. Figure 4-1 shows how well different simulant grain size curves match with the lunar soils from Apollo 11 and 12.

The LSS (40/60) was one of the earliest simulants used. The 40/60 refers to the ratio of crushed basalt to sand. After the return of lunar samples from Apollo 11 and 12, the mix was revised in order to achieve a better match to the grain size distribution [LSS (11/12)]. The LSS (WES) mix was developed in early lunar roving vehicle studies by the US Army Corps of Engineers (Costes et al., 1971).

4.2. APPLICATIONS OF SIMULANTS

Laboratory cone penetration resistance tests were conducted on the simulants in order to assist in back-calculating soil properties from insertion of poles, tubes and staffs on the Apollo 11 and 12 missions. The laboratory tests used were the same as the penetration tests discussed in Chapter 3.2 (Figure 3-9). Typical results of these tests show the penetration resistance and resistance gradient as functions of the bulk density, relative density and void ratio. For a given penetration resistance there is quite a wide variation in computed void ratio among the various lunar simulants (Figure 4-2). The LSS (11/12 MIX)'s response to penetration is significantly different than the other simulants. This can be attributed to the fact that it is the most recent mix, showing the results of changes due to data available from returned lunar samples.

Yuma sand and the LSS (11/12) mix were also used in penetration tests on board U.S. Air Force KC-135 aircraft used to induce various gravity conditions. Tests took place in 1/6-gravity dives and 2g climbs, Figure 4-3 (Costes et al. 1971). These results show the importance of calibrating cone resistance, q_c , the actual gravitational acceleration on the moon.

As discussed previously core tube geometry has an enormous effect on the quality of samples returned to earth. Carrier et al. (1971,1972b) conducted a study to assess the amount disturbance in recovered Apollo core tubes. Specifically, the differences between depths seen in core tube samples, and actual depths in the lunar surface. For the purposes of a study, a mixture of League City sand (65%) and Kaolinite clay (35%) was used. It was decided

that, for this study, matching the cohesive and frictional properties of the lunar soil was more important than the effect of grain size differences due to the presence of Kaolinite in the mix.⁶ The water content, $w = 0.6\%$ by weight and the density $\rho = 1.33 \text{ g/cm}^3$. A comparison of the properties of the lunar and simulant soils is shown in Table 4-1.

Defined layers were created in the simulant by adding manganese dioxide, a black powder, at different depths (Carrier et al., 1971). The estimations were made by simply comparing the location of the dark, manganese oxide layers in the tubes, to their locations in the test area. Figure 4-4 displays a testing core with the defined dark and light regions. With similar techniques, new sampler designs could be tested and improved.

Lunar simulants were also used for with laboratory tests on retrieved lunar soil. A ground basaltic simulant (Carrier et al., 1972a) was tested using the same direct shear apparatus discussed in Chapter 3. It was found that the shear strength of the lunar soil was significantly less than the simulant, While the results were not expected to agree exactly, the differences were higher than expected. Lunar soil was found to be about 65% weaker than the basaltic simulant at the same void ratio. It has been theorized that the large difference is due to the existence of weakly cemented particles in the lunar soil, such as small breccia particles and agglutinates. The crushing and breaking of these weak bonds could be what causes the sharp difference in strength (Carrier et al., 1972a).

⁶ Rationale for saturated soil based on assumption that Terzaghi principle of effective stress is valid.

More recent studies of lunar simulants have sprung from the increasing possibility of future lunar base construction (Willman et al., 1995a; Willman et al., 1995b; Perkins and Madson, 1996). Since the last of the Apollo missions (1972), there have been substantial advances in the understanding of soil behavior and improvements in the replication of lunar soil properties.

The lunar simulant JSC-1 was developed at Johnson Space Center to fill the need for studies concerning lunar construction, foundation design and mining (Willman et al., 1995a). A basaltic ash deposit near Flagstaff, Arizona was chosen to be the basic component of the simulant. Again, the basaltic content of the simulant gives it a specific gravity of approximately 2.9, compared to 3.1 for lunar soils. JSC-1 was designed to have a similar grain size distribution to that of lunar soils, Figure 4-5.

Texas A&M University ran CD (Consolidated Drained) Triaxial Tests on the simulant for comparisons of strength parameters. The soil was consolidated to typical values of in-situ density for lunar soils. For all tests, $\phi = 45^\circ$ and $c \leq 1.0$ kPa (Figure 4-6).

The physical properties of the soil grains were also taken into account in the design of the JSC-1 simulant. Values of elongation, the ratio of particle length to width, were compared to determine the relative similarity of soil particles. Similarly, comparisons of particle aspect ratio, the ratio of minor to major axis, were made (Willman et al 1995). A summary of the properties of JSC-1 and lunar soil is made in Table 4-2.

Careful choosing of new lunar soil simulants is extremely beneficial in the design of future construction equipment. Due to the lunar surface being

constantly bombarded by solar wind and small particles, underground structures are a strong possibility in design. Problems arise in the design of excavation equipment due to the inability to test equipment at the site (Willman et al. 1995b). Payload size on rockets and shuttles to the moon are limited in size. Any equipment transported to the lunar surface for use in construction will have to be specifically tailored to be efficient in that location. Proper matching of the physical and mechanical properties of lunar soil with simulants gives researches and designers the ability to solve these problems.

FIGURES

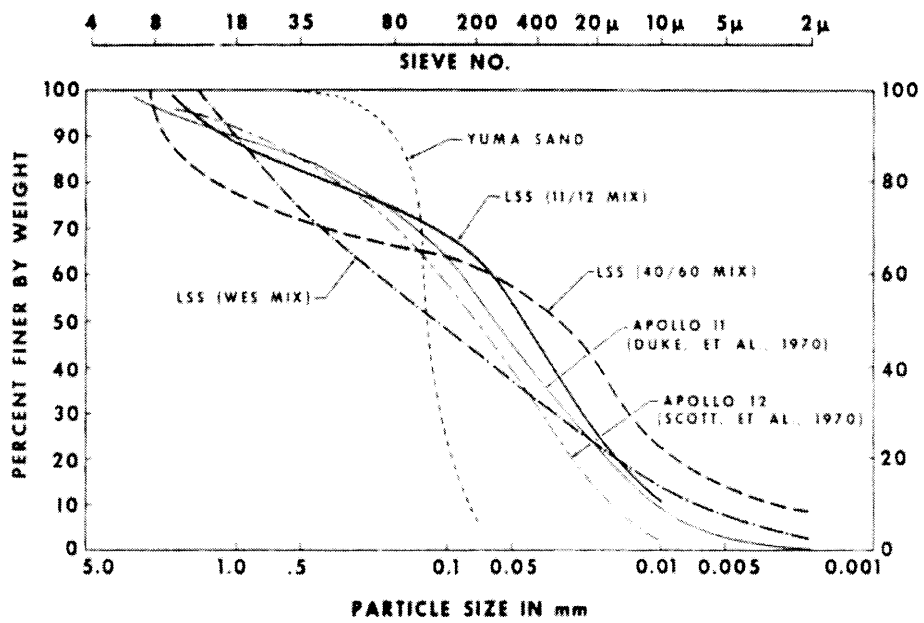


Figure 4-1 - Comparison of Grain Size Curves for Apollo samples and simulants. (Costes et al., 1971)

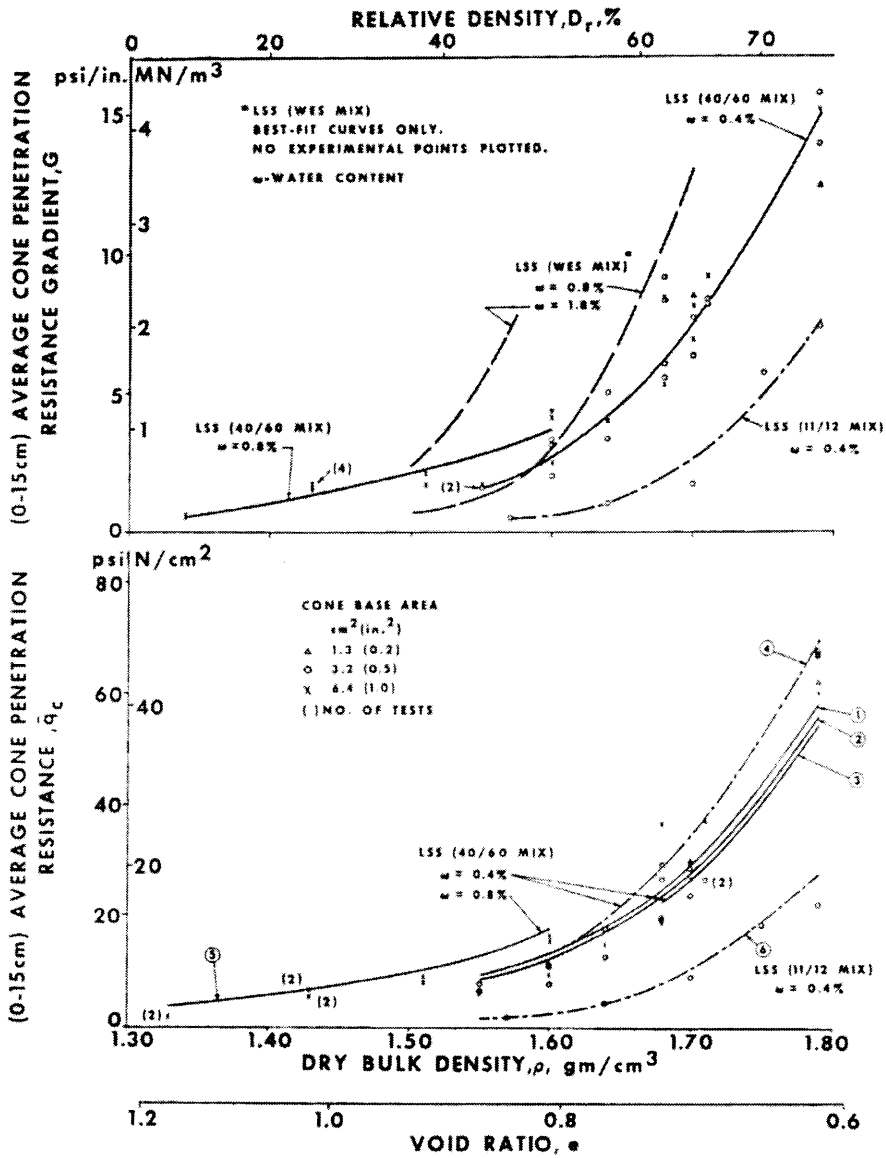


Figure 4-2 - Penetration Test Results for Lunar Soil Simulants. (Costes et al., 1971)

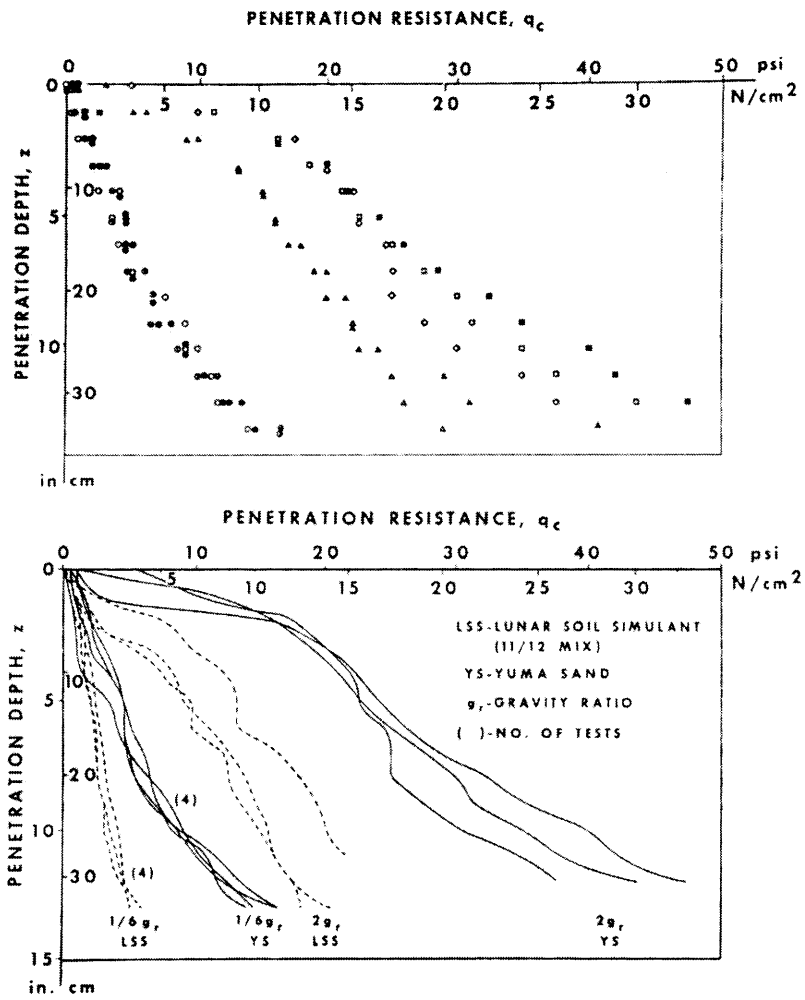


Figure 4-3 - Results of varying g levels on penetration resistance of lunar soil simulants. (Costes et al., 1971)

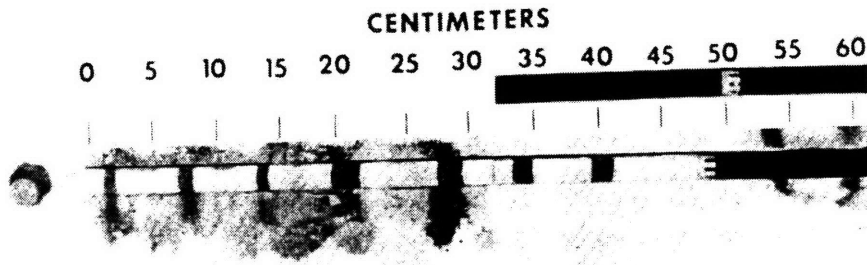


Figure 4-4 - Results of sample disturbance tests with a lunar soil simulant. Note the curvature of the dark layers on the left, indicating insertion disturbance due to frictional effects. (Carrier et al., 1971)

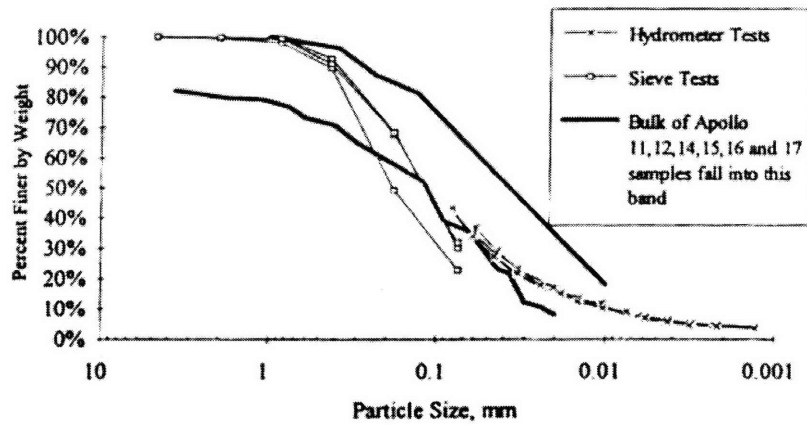


Figure 4-5 - Particle Size Distribution of JSC-1 compared to lunar soils. JSC-1 data plotted from Hydrometer and Sieve tests. (Willman et al., 1995)

Triaxial Compression Data
Density = 1.65 gm/cm³

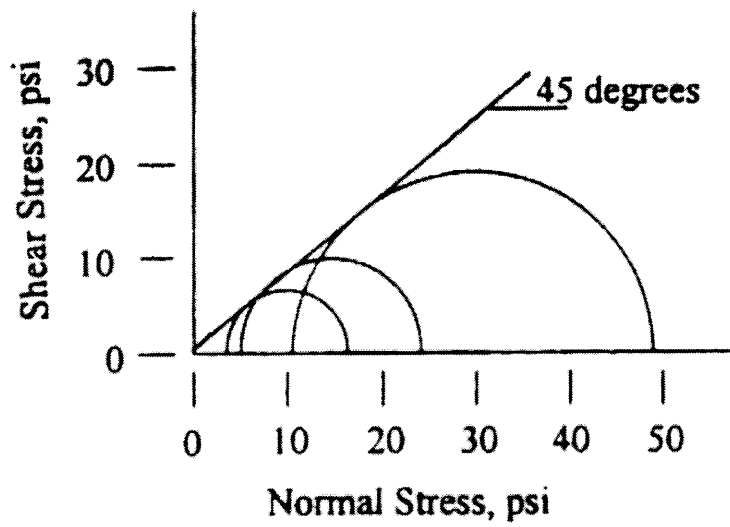


Figure 4-6 Mohr's Circles for JSC-1 CD triaxial compression test. (Willman et al., 1995)

TABLES

Property	Lunar Soil	Terrestrial Simulant
Friction Angle	35° - 37°	37°
Cohesion (kN/m ²)	0.343 - 0.686	1.933
Bulk Density (g/cm ³)	1.6 - 2.0	1.33
Unit Weight (kN/m ³)	2.61 - 3.26	13.05
Cohesion /Unit Weight (cm)	10.5 - 26.3	14.8

Table 4-1 - Summary of the soil properties of lunar soils and lunar soil simulant. Unit weights calculated for in-situ gravity conditions. (Carrier et al., 1971).

Parameter	JSC-1	Lunar Soil
Specific Gravity	2.91	3.1
Friction Angle	45°	30 -50 °
Cohesion	< 1.0 kPa	0.1 - 1.0 kPa
Elongation	1.69	1.31 - 1.39
Aspect Ratio	0.68	0.4 - 0.7

Table 4-2 - Properties of JSC-1 and Lunar Soil (Willman et al., 1995)

5. SUMMARY AND CONCLUSIONS

This thesis summarized briefly the history and events that have created lunar regolith and the subsequent investigations of lunar soil properties dating from the Surveyor and Apollo test programs. The most detailed understanding of lunar soil has been derived from samples returned to earth by the five Apollo missions that successfully landed on the moon. We now know that lunar soil is similar in size and shape to an angular terrestrial well-graded silty sand to sandy silt (SW-SM to ML in the USCS classification system). Furthermore, we know that the soil exhibits a small amount of cohesion, commonly attributed to solar wind bombardment causing an electrostatic surface charge. Estimates of engineering properties, while subject to a degree of uncertainty, are bounded within well-defined ranges. The lack of water, atmosphere, man and other common terrestrial factors on the lunar surface lead to relatively low levels of spatial variability in soil properties. However, some questions remain unanswered.

The precise location of lunar bedrock is still relatively unknown. Although, surface geophysical techniques have managed to yield information concerning the depth of dense consolidated layers, approximately 8.5 m at the Fra Mauro site. Furthermore, while the nature and magnitude of cohesive strength components have been measured, their origin remains speculative and has not been replicated in tests with terrestrial simulant soils.

The Space Exploration Initiative (SEI) was established in 1991 for the purposes of outlining America's goals for the future of such undertakings as lunar settlement and Martian exploration (Jolly, 1994). The increasing possibility that lunar construction could take place in the near future has motivated the recent research on lunar simulants (Willman et al., 1995a; Willman et al., 1995b; Perkins and Madson, 1996) as discussed in Chapter 4.2. Further, studies are currently in progress in the design of instrumentation, sampling equipment, etc. for future explorations of Mars, and are based heavily on the experience with lunar soils.

It is interesting to note that the nature of Martian soil has also been estimated to be granular, silt sized, and having the existence of an upper crust of cemented soil (Chua and Johnson, 1998). Cold region lunar and Martian soil studies conducted by Chua and Johnson (1998) used the lunar soil simulant JSC-1 as the model for both. The implications of similarity between lunar and Martian soils would give scientists firm footing, based on the accumulation of lunar soil data, with which to begin design tool.

Lunar base construction an engineering problem closer to realization than human exploration of the Martian surface. Design and construction of a lunar base is feasible with the current state of knowledge concerning lunar soil mechanics. However, the uncertainty involved would undoubtedly lead to poor or over-designed equipment and structural components. The first case is clearly unacceptable due to the inherent danger involved in any construction process and the possibility of failure or loss of life on the lunar surface. The second case is less dramatic, but would lead to excess costs and wasted payload space in the shuttle or rocket. In any case, a full-scale geotechnical exploration

of a chosen site is recommended. This exploration should include, but not be limited to large-scale trenching, in-situ penetration, deep core sampling and surface geophysical techniques. Furthermore, testing for shear strength and deformation parameters should be conducted on the lunar surface, perhaps in a temporary laboratory, for the most accurate results. Geophysical exploration is a field in which large advances have been made since its use in the Apollo missions. Newer, more accurate techniques would be extremely useful for extensive profiling of lunar soil. Accurate data concerning strength parameters must be obtained for the design of the foundations, anchors, underground facilities, etc.

The current knowledge of lunar soils reflects the culmination of more than 40 years of observation, testing, exploration and laboratory study. Lunar development is more a question of when than how or why. The lessons learned in the process are almost as valuable as the knowledge of lunar soils itself. Future missions to the moon will use much more sophisticated computer controlled technology for exploration, with most of the major uncertainties in soil properties resolved by data from the Surveyor and Apollo programs. Sophisticated exploration will undoubtedly yield more comprehensive information than was obtained throughout the entire Apollo program. Furthermore, the application of lunar soil exploration knowledge to Martian exploration offers scientists and engineers a degree of confidence that those involved in the Surveyor and Apollo programs sorely lacked.

REFERENCES

- Carrier W.D. III, Bromwell L.G., Martin R.T. (1972a) Strength and compressibility of returned lunar soil. *Proceedings of the Third Lunar Science Conference, Geochim. Cosmochim. Acta Suppl. 3, Vol. 3, pp. 3223-3234.* MIT Press
- Carrier W.D. III, Johnson S.W., Carrasco L.H., Schmidt R. (1972b) Core sample depth relationships: Apollo 14 and 15. *Proceedings of the Third Lunar Science Conference, Geochim. Cosmochim. Acta Suppl. 3, Vol. 3, pp. 3213-3221*
- Carrier W.D. III, Johnson S. W., Werner R. A., Schmidt R. (1971) Disturbance in samples recovered with the Apollo core tubes. *Proceedings of the Second Lunar Science Conference, Vol 3, pp. 1959-1972.* MIT Press.
- Christensen E.M., Batterson S.A., Benson H.E., Chandler C.E., Jones R.H., Scott R.F., Shipley E.N, Sperling F.B., Sutton G.H. (1967) Lunar Surface Mechanical Properties – Surveyor 1. *Journal of Geophysical Research, Vol. 72, No. 2, pp. 801 – 813.*
- Chua K.M., Jonshon S.W. (1998) Martian and Lunar Cold Region Soil Mechanics Considerations. *Journal of Aerospace Engineering, Vol. 11, No. 4, pp. 138-147.*

- Costes N.C., Cohron G.T., Moss D.C. (1971) Cone penetration resistance test - an approach to evaluating in-place strength and packing characteristics of lunar soils. *Proceedings of the Second Lunar Science Conference*, Vol. 3, pp. 1973-1987. MIT Press.
- Costes N.C., Mitchell J.K. (1970) Apollo 11 soil mechanics investigation. *Proceedings of the Apollo 11 Lunar Science Conference*, Vol. 3, pp. 2025-2044.
- Das B.M. (1998) Principles of Geotechnical Engineering. 4th ed. PWS Publishing Company. Boston, MA.
- FrondeLL J.W. (1975) Lunar Mineralogy. John Wiley & Sons, Inc. New York, NY.
- Fryxell R., Anderson D., Carrier W.D. III, Greenwood W., Heiken G. (1970) Apollo 11 drive-tube core samples: an initial physical analysis of lunar surface sediment. *Proceedings of the Apollo 11 Lunar Science Conference*, Vol. 3, pp. 2121-2126.
- Guest J.E., Greeley R. (1977) Geology on the moon. Wykeham Publications Ltd. London, England.
- Heiken G., Vaniman D., French B.M. (1991) Lunar Sourcebook: a user's guide to the moon. Cambridge University Press. New York, NY.
- Houston W.N., Mitchell J.K. (1971) Lunar core tube sampling. *Proceedings of the Second Lunar Science Conference*, Vol. 3, pp. 1953-1958. MIT Press.

- Houston W.N., Hovland H.J., Mitchell J.K., Namiq L.I. (1972) Lunar soil porosity and its variation as estimated from footprints and boulder tracks. *Proceedings of the Third Lunar Science Conference, Geochim. Cosmochim. Acta Suppl.* 3, Vol. 3, pp. 3255-3263. MIT Press.
- Jolly S.D., Happel J., Sture S. (1994) Design and Construction of Shielded Lunar Outpost. *Journal of Aerospace Engineering*, Vol. 7, No. 4, pp. 417-434.
- Levinson A.A., Taylor S.R. (1971) Moon Rocks and Minerals. Pergamon Press. New York, NY.
- Mitchell J.K., Bromwell L.G., Carrier W.D. III, Costes N.C., Scott R.F. (1972b) Soil Mechanics Properties at the Apollo 14 Site. *Journal of Geophysical Research*, Vol. 77, No. 29, pp. 5641-5664.
- Mitchell J.K., Houston W.N., Scott R.F., Costes N.C., Carrier W.D. III, Bromwell L.G. (1972a) Mechanical properties of lunar soil: Density, porosity, cohesion, and angle of internal friction. *Proceedings of the Third Lunar Science Conference, Geochim. Cosmochim. Acta Suppl.* 3, Vol. 3, pp. 3235-3253. MIT Press.
- Mutch T.A. (1970) Geology of the moon: A stratigraphic view. Princeton University Press. Princeton, NJ.
- Perkins S.W., Madson C.R. (1996) Mechanical and Load Settlement Characteristics of Two Lunar Soil Simulants. *Journal of Aerospace Engineering*, Vol. 9, No.1, pp. 1-9.

Scott R.F. (1967) Soil Mechanics Surface Sampler Experiment for Surveyor. *Journal of Geophysical Research*, Vol. 72, No. 2, pp. 827-830.

Scott R.F. (1973) Lunar Soil Mechanics. *Proceedings from the Eighth International Conference on Soil Mechanics Foundation Engineering, Moscow*, Vol. 4, Iss. 2, pp 177-190.

Scott R.F. (1987) Failure. *Geotechnique* 37, No. 4, pp. 423-466.

Scott R.F., Carrier W.D. III, Costes N.C., Mitchell J.K. (1971) Apollo 12 Soil Mechanics Investigation. *Geotechnique* 21, No. 1, pp. 1-14.

Scott R.F., Roberson F.I. (1968) Soil Mechanics Surface Sampler: Lunar Surface Tests, Results, and Analyses. *Journal of Geophysical Research*, Vol. 73, No. 12, pp. 4045-4080.

Willman B.M., Boles W.W. (1995b) Soil-Tool Interaction Theories As They Apply To Lunar Soil Simulant. *Journal of Aerospace Engineering*, Vol. 8, No.2, pp. 88-99.

Willman B.M., Boles W.W., Mckay D.S., Allen C.C. (1995a) Properties of Lunar Soil Simulant JSC-1. *Journal of Aerospace Engineering*, Vol. 8, No. 2, pp. 77-87.

WWW.ASTM.ORG

WWW.NASA.GOV